Atmos. Chem. Phys., 18, 5567–5588, 2018
https://doi.org/10.5194/acp-18-5567-2018

Atmospheric Chemistry and Physics
Open Access
EGU

Revisiting the contribution of land transport and shipping emissions to tropospheric ozone

Mariano Mertens[1], **Volker Grewe**[1,2], **Vanessa S. Rieger**[1,2], **and Patrick Jöckel**[1]

[1]Deutsches Zentrum für Luft- und Raumfahrt, Institut für Physik der Atmosphäre, Oberpfaffenhofen, Germany
[2]Delft University of Technology, Aerospace Engineering, Section Aircraft Noise and Climate Effects, Delft, the Netherlands

Correspondence: Mariano Mertens (mariano.mertens@dlr.de)

Received: 9 August 2017 – Discussion started: 12 October 2017
Revised: 22 March 2018 – Accepted: 23 March 2018 – Published: 24 April 2018

Abstract. We quantify the contribution of land transport and shipping emissions to tropospheric ozone for the first time with a chemistry–climate model including an advanced tagging method (also known as source apportionment), which considers not only the emissions of nitrogen oxides (NO_x, NO, and NO_2), carbon monoxide (CO), and volatile organic compounds (VOC) separately, but also their non-linear interaction in producing ozone. For summer conditions a contribution of land transport emissions to ground-level ozone of up to 18 % in North America and Southern Europe is estimated, which corresponds to 12 and 10 nmol mol^{-1}, respectively. The simulation results indicate a contribution of shipping emissions to ground-level ozone during summer on the order of up to 30 % in the North Pacific Ocean (up to 12 nmol mol^{-1}) and 20 % in the North Atlantic Ocean (12 nmol mol^{-1}). With respect to the contribution to the tropospheric ozone burden, we quantified values of 8 and 6 % for land transport and shipping emissions, respectively. Overall, the emissions from land transport contribute around 20 % to the net ozone production near the source regions, while shipping emissions contribute up to 52 % to the net ozone production in the North Pacific Ocean. To put these estimates in the context of literature values, we review previous studies. Most of them used the perturbation approach, in which the results for two simulations, one with all emissions and one with changed emissions for the source of interest, are compared. For a better comparability with these studies, we also performed additional perturbation simulations, which allow for a consistent comparison of results using the perturbation and the tagging approach. The comparison shows that the results strongly depend on the chosen methodology (tagging or perturbation approach) and on the strength of the perturbation. A more in-depth analysis for the land transport emissions reveals that the two approaches give different results, particularly in regions with large emissions (up to a factor of 4 for Europe). Our estimates of the ozone radiative forcing due to land transport and shipping emissions are, based on the tagging method, 92 and 62 mW m^{-2}, respectively. Compared to our best estimates, previously reported values using the perturbation approach are almost a factor of 2 lower, while previous estimates using NO_x-only tagging are almost a factor of 2 larger. Overall our results highlight the importance of differentiating between the perturbation and the tagging approach, as they answer two different questions. In line with previous studies, we argue that only the tagging approach (or source apportionment approaches in general) can estimate the contribution of emissions, which is important to attribute emission sources to climate change and/or extreme ozone events. The perturbation approach, however, is important to investigate the effect of an emission change. To effectively assess mitigation options, both approaches should be combined. This combination allows us to track changes in the ozone production efficiency of emissions from sources which are not mitigated and shows how the ozone share caused by these unmitigated emission sources subsequently increases.

Published by Copernicus Publications on behalf of the European Geosciences Union.

1 Introduction

Ozone in the troposphere has several well-known effects: it contributes to global warming due to its radiative properties (e.g. Stevenson et al., 2006; Myhre et al., 2013), and large concentrations of ozone are harmful to humans and to plants (e.g. World Health Organization, 2003; Fowler et al., 2009). In addition, ozone is an important source for the OH radical, which controls the cleansing capacity of the troposphere (e.g. the lifetime of methane; Naik et al., 2013). Due to these different effects ozone is a central species of atmospheric chemistry (Monks et al., 2015).

Two important sources of ozone exist in the troposphere: downward transport from the stratosphere and in situ production from precursor emissions (e.g. Lelieveld and Dentener, 2000; Grewe, 2004). The most important precursors of ozone are carbon monoxide (CO), methane (CH_4), volatile organic compounds (VOC), and nitrogen oxides ($NO_x = NO + NO_2$; e.g. Haagen-Smit, 1952; Crutzen, 1974; Monks, 2005). These precursors have anthropogenic and natural sources. Important natural sources of VOCs are biogenic emissions (e.g. Guenther et al., 1995), while NO_x is emitted by lightning (e.g. Schumann and Huntrieser, 2007) and soil (e.g. Yienger and Levy, 1995; Vinken et al., 2014). Anthropogenic sources of ozone precursors, on the other hand, include emissions from industry, land transport (containing the sources road traffic, inland navigation, and railways; e.g. Uherek et al., 2010), and shipping (e.g. Eyring et al., 2010). With respect to the influence of different emission sources on ozone itself, typically two different questions are of interest (e.g. Wang et al., 2009; Grewe et al., 2010; Clappier et al., 2017).

- How sensitively does ozone respond to changes in a specific emission source (sensitivity study)?
- How large is the contribution of different emission sources to ozone (source apportionment)?

Sensitivity studies are important to investigate the influence of an emission change on, for instance, ozone. Often, the so-called perturbation approach has been applied, in which the results of two (or more) simulations are compared: one reference simulation with all emissions and a sensitivity simulation with perturbed emissions. Source apportionment, in contrast, is important to attribute different emission sources to climate impact (such as radiative forcing) or extreme ozone events. Source apportionment studies often use tagged tracers in order to estimate contributions of different emission sources, for instance, to ozone. In this tagging approach, additional diagnostic species are introduced which follow the reaction pathways of the emissions from different sources (e.g. Lelieveld and Dentener, 2000; Dunker et al., 2002; Grewe, 2004; Gromov et al., 2010; Butler et al., 2011; Grewe et al., 2012; Emmons et al., 2012; Kwok et al., 2015). Other methods exist for both type of studies (e.g. sensitivity and source apportionment), which we neglect here for simplicity (see e.g. Clappier et al., 2017).

In a linear system, both perturbation and tagging lead to the same result (e.g. Grewe et al., 2010; Clappier et al., 2017). The O_3 chemistry, however, is highly non-linear. Therefore, both approaches lead to different results, not because of uncertainties in the method, but because they give answers to different questions. Here, we use the following wording to discriminate between these two types of questions and methods, acknowledging that other authors may use them differently: the impact of a source is calculated by using the sensitivity method (here the perturbation approach), while the contribution is calculated using a source apportionment method (here the tagging approach; e.g. Wang et al., 2009; Grewe et al., 2010; Clappier et al., 2017). Accordingly, the impact indicates the effect of an emissions change, while the contribution enables an attribution of ozone (and associated radiative forcing) to specific emissions sources.

In the past, many studies have been performed to estimate the impact of road traffic emissions (but not the total land transport effect; e.g. Granier and Brasseur, 2003; Niemeier et al., 2006; Matthes et al., 2007; Hoor et al., 2009; Koffi et al., 2010) on the global scale. However, only a few studies exist that estimate the contribution of road traffic emissions to ozone: Dahlmann et al. (2011) and Grewe et al. (2012) used a tagging approach considering only NO_x. Further, these studies focused mainly on globally averaged tropospheric ozone columns and associated radiative forcings without regional quantifications of the contribution. Similarly, for the shipping sector previous studies focused on the calculation of the impact (e.g. Lawrence and Crutzen, 1999; Eyring et al., 2007; Hoor et al., 2009; Koffi et al., 2010; Holmes et al., 2014). Only Dahlmann et al. (2011) reported results of O_3 due to shipping emissions using a NO_x-only tagging approach.

It is well known that the impact is usually smaller compared to the contribution (e.g. Grewe et al., 2012, 2017; Emmons et al., 2012). Furthermore, impacts are usually not additive. This means that the ozone changes (impacts) which are calculated for different emission sources by perturbing one of the emission sources is not the same as perturbing all of the emission sources at the same time. This holds not only for the ozone concentration, but also for the associated ozone radiative forcing. As land traffic and shipping emissions are important sources of ozone precursors, it is very important to calculate not only their impact on ozone, but also the contribution of these emissions to ozone in detail. Further, our approach tags not only NO_x and VOC individually, but also both ozone precursors concurrently for the first time (Grewe et al., 2017). Therefore, the goal of the present study is twofold: first we review estimates of land transport and shipping emissions in terms of their contribution to and impact on tropospheric ozone and the resulting radiative forcing. Second, we present new results analysing the contribution of land transport and shipping emissions in de-

tail using a tagging approach. These new results quantify for the first time the contributions of the considered emissions on (ground-level) ozone in detail. Further, we also report results using a perturbation approach in a consistent manner to bridge the gap between previous studies and our new results. This allows for a detailed comparison of the impact and contribution, as well as the associated ozone radiative forcings, between the perturbation approach, the NO_x tagging, and NO_x and VOC tagging.

The paper is organized as follows: in Sect. 2 we give an overview of the model system used and describe the applied set-up. In Sect. 3 we analyse our simulation results with respect to the contribution vs. the impact of land transport and shipping emissions to ground-level ozone, including a detailed overview and discussion of the results from previous studies. In Sect. 4 we compare our results using the perturbation and the tagging approach in more detail. Section 5 gives more detailed insights into the tropospheric ozone budget. The contribution of the land transport and shipping emissions to radiative forcing due to ozone is analysed in Sect. 6, while Sect. 7 presents a discussion about the uncertainties associated with the tagging and perturbation approaches.

2 Model description and set-up

2.1 Model description

We applied the ECHAM/MESSy Atmospheric Chemistry (EMAC) chemistry–climate model (Jöckel et al., 2006, 2010, 2016) equipped with the TAGGING technique described by Grewe et al. (2017). EMAC uses the second version of the Modular Earth Submodel System (MESSy2) to link multi-institutional computer codes. The core atmospheric model is the 5th generation European Centre Hamburg general circulation model (ECHAM5 Roeckner et al., 2006). For the present study we applied EMAC (ECHAM5 version 5.3.02, MESSy version 2.52) in the T42L90MA resolution, i.e. with a spherical truncation of T42 (corresponding to a quadratic Gaussian grid of approximately 2.8 by 2.8° in latitude and longitude) with 90 vertical hybrid pressure levels up to 0.01 hPa. The simulation set-up is almost identical to the one of the simulation *RC1SD-base-10a* described in detail by Jöckel et al. (2016) alongside an evaluation of the resulting model simulation. Therefore, we describe only the most important details and differences. A comparison with the results of the simulation presented here and the *RC1SD-base-10a* is part of the Supplement of the present paper.

The chosen simulation period covers the years 2004 to 2010. The years 2004–2005 serve as a spin-up, while the years 2006–2010 are analysed. Initial conditions for the trace gas distribution were taken from the *RC1SD-base-10a* simulation (Jöckel et al., 2016). Lightning NO_x is parameterized after Grewe et al. (2002) with global total emissions of $\approx 4.5\,\mathrm{Tg\,(N)\,a^{-1}}$. Emissions of NO_x from soil and biogenic C_5H_8 emissions were calculated using the MESSy submodel ONEMIS (Kerkweg et al., 2006) using parameterizations based on Yienger and Levy (1995) for soil NO_x and Guenther et al. (1995) for biogenic C_5H_8. The applied gas-phase mechanism in MECCA (Sander et al., 2011) incorporates the chemistry of ozone, methane, and odd nitrogen. Alkanes and alkenes are considered up to C4, while the oxidation of C_5H_8 and some non-methane hydrocarbons (NMHCs) are described with the Mainz Isopren Mechanism version 1 (von Kuhlmann et al., 2004). Further, heterogeneous reactions in the stratosphere (submodel MSBM; Jöckel et al., 2010) and aqueous-phase chemistry and scavenging (SCAV; Tost et al., 2006) are included. Emissions of methane (CH_4) are not considered explicitly. Instead pseudo-emissions are calculated using the submodel TNUDGE (Kerkweg et al., 2006). TNUDGE relaxes mixing ratios in the lowest model layer towards observations using Newtonian relaxation (see also Jöckel et al., 2016).

EMAC is "nudged" by Newtonian relaxation of temperature, divergence, vorticity, and the logarithm of surface pressure (Jöckel et al., 2006) towards ERA-Interim (Dee et al., 2011) reanalysis data. Also, the sea surface temperature and sea ice coverage are prescribed as transient time series from ERA-Interim. To allow for identical meteorological conditions in sensitivity experiments with changed emissions, the quasi-chemistry transport model mode (QCTM mode; Deckert et al., 2011) of EMAC was used. In this mode, climatologies of the radiative active trace gases are prescribed for the calculation of the radiation. Further, climatologies are used for processes which couple the chemistry and the hydrological cycle. The applied climatologies are monthly average values taken from the *RC1SD-base-10a* simulation.

2.2 Tagging method for source attribution

The tagging is performed using the MESSy TAGGING submodel described in detail by Grewe et al. (2017). This tagging method is an accounting system following the relevant reaction pathways and applies the generalized tagging method introduced by Grewe (2013). This method diagnoses the contributions of different categories to the regarded species without influencing the full chemistry. A prerequisite for this method is a complete decomposition of the source terms, e.g. emissions, of the regarded species in N unique categories. As a consequence of the complete decomposition, the sum of the contributions of all tagged categories of one species equals the total concentration of this species (i.e. the budget is closed):

$$\sum_{\mathrm{tag}=1}^{N} \mathrm{O_3^{tag}} = \mathrm{O_3}. \quad (1)$$

As an example of this method, consider the production of O_3 by the reaction of NO with an organic peroxy radical

Table 1. Description of the different categories as used by the TAGGING submodel.

Tagging categories	Description
Land transport	Emissions of road traffic, inland navigation, railways (IPCC code 1A3b_c_e)
Anthropogenic non-traffic	Sectors energy, solvents, waste, industries, residential, agriculture
Ship	Emissions from ships (IPCC code 1A3d)
Aviation	Emissions from aircraft
Lightning	Lightning NO_x emissions
Biogenic	Online-calculated isoprene and soil NO_x emissions, offline emissions from biogenic sources and agricultural waste burning (IPCC code 4F)
Biomass burning	Biomass burning emissions
CH_4	Degradation of CH_4
N_2O	Degradation of N_2O
Stratosphere	Downward transport from the stratosphere

(RO_2) to NO_2 and the organic oxy radical (RO):

$$NO + RO_2 \longrightarrow NO_2 + RO. \quad (R1)$$

For this reaction the tagging approach leads to the following fractional apportionment (see Eqs. 13 and 14 in Grewe et al., 2017, for a detailed example):

$$P_{R1}^{tag} = \frac{1}{2} P_{R1} \left(\frac{NO_y^{tag}}{NO_y} + \frac{NMHC^{tag}}{NMHC} \right). \quad (2)$$

In this case the variables marked with ^{tag} represent the tagged production rate of O_3 by Reaction (R1) (P) as well as the tagged families of NO_y and NMHC (details given below) of one individual category (e.g. land transport). Accordingly, the fractional apportionment is inherent to the method based on a combinatorial approach, which decomposes every regarded reaction into all possible combinations of reacting tagged species. This takes into account the specific reaction rate constant from the full chemistry scheme (implicitly by the production and loss rates from the chemistry solver). The chemical mechanism including all diagnosed production and loss rates for the tagging method are part of the Supplement. The analysed production and loss rates in Sect. 5 are calculated in accordance with Eqs. (13) and (14) of Grewe et al. (2017).

The applied method considers 10 categories (detailed definition is given in Table 1). To minimize the needed amount of memory and computational performance, not every individual species is tagged. Instead a family concept is chosen. The following families are taking into account: O_3, NO_y, PAN, NMHC and CO. Additionally, OH and HO_2 are tagged by using a steady-state approach. In the following, we denote absolute contributions of land transport and shipping emissions to ozone diagnosed with the tagging method as O_3^{tra} and O_3^{shp}, respectively.

2.3 Radiative forcing

The radiative forcing (RF) of ozone is defined as the difference in the net radiative fluxes caused by a change (e.g. between two time periods like pre-industrial and present day; Myhre et al., 2013). Here, we are interested in the contribution of land transport and shipping to this RF. Due to the non-linearities in the ozone chemistry (see also Sect. 4), we estimate the contribution of the land transport and shipping emissions to ozone and then calculate the RF of these O_3 shares individually. This approach is consistent with the IPCC RF definition, since the sum of all individual RF contributions approximately equals the total RF (for a detailed example, see Dahlmann et al., 2011).

Thus, to calculate the O_3 RFs of land traffic and shipping emissions, additional simulations were performed by applying the stratospheric adjusted radiative forcing concept (e.g. Hansen et al., 1997; Stuber et al., 2001; Dietmüller et al., 2016). For this, monthly mean fields of the simulation *RC1SD-base-10a* are used as input data for the radiation scheme, except for O_3, which stems from the *BASE* simulation. Calculations of the RF based on the results of the tagging approach in accordance with Dahlmann et al. (2011) were performed as follows.

1. Based on the results of the *BASE* simulation, monthly mean values of $\Delta_T^{tra} = O_3 - O_3^{tra}$ and $\Delta_T^{shp} = O_3 - O_3^{shp}$ were calculated. Δ_T^{tra} and Δ_T^{shp} correspond to the share of O_3 excluding O_3 from land transport and shipping emissions, respectively.

2. Multiple radiation calculations (Dietmüller et al., 2016) were performed, calculating the radiative flux of Δ_T^{tra}, Δ_T^{shp}, and O_3. The O_3 RFs of land transport and shipping emissions using the tagging approach are then calculated as follows:

$$RF_{O3tra}^{tagging} = rflux(O_3) - rflux\left(\Delta_T^{tra}\right), \quad (3)$$

$$RF_{O3shp}^{tagging} = rflux(O_3) - rflux\left(\Delta_T^{shp}\right), \quad (4)$$

with rflux being the net radiative fluxes calculated for the respective quantity. Accordingly, the calculated RFs

Table 2. Average (2006–2010) annual total emissions of CO (in Tg (CO) a^{-1}), NO_x (in Tg (N) a^{-1}), and NMHC (in amount of carbon) of the most important emission categories. The category "other" contains the emissions of the sectors biomass burning, agricultural waste burning, and other biogenic emissions.

	CO (Tg (CO) a^{-1})	NMHC (Tg (C) a^{-1})	NO_x (Tg (N) a^{-1})
Land transport	152	17	10
Shipping	1	2	6
Anthropogenic non-traffic	411	73	17
Soil NO_x			6
Lightning NO_x			5
Biogenic C_5H_8		493	
Other	416	15	5

measure the flux change caused by the ozone share of land transport and shipping emissions, respectively.

Calculating the RFs based on the results of the perturbation approach is similar to Myhre et al. (2011). First, ΔO_{3tra} and ΔO_{3shp} are calculated by taking the difference between the unperturbed (*BASE*, see below) and the perturbed simulations (*LTRA95* or *SHIP95*):

$$\Delta O_3 = \left({O_3}^{\text{unperturbed}} - {O_3}^{\text{perturbed}} \right) \cdot 20. \quad (5)$$

As we consider 5 % perturbations (e.g. the emissions of land transport and shipping are decreased by 5 %; see Sect. 2.4) these differences are scaled by a factor of 20 to yield a 100 % perturbation. To calculate the RFs using the perturbation approach, ΔO_{3tra} and ΔO_{3shp} are then treated as described above for Δ_T^{tra} and Δ_T^{shp}. These RFs are called $RF_{\Delta O3tra}^{perturbation}$ and $RF_{\Delta O3shp}^{perturbation}$, respectively. Accordingly, the method to calculate the RFs of the O_3 shares analysed by the perturbation and the tagging approach are the same. The differences between $RF_{O3tra}^{perturbation}$ and $RF_{O3tra}^{tagging}$ (and the same for shipping) arise only due to differences in the differently calculated O_3 shares.

The benefit of using the contribution of an emission source (in contrast to using the impact of the emission source) is that for the contribution the sum of the individual radiative forcings is equal to the total RF; i.e. $\sum_i^n RF^i \approx RF$ with RF^i being the radiative forcings of the individual categories i of n total categories. This holds for the perturbation approach (Dahlmann et al., 2011; Grewe et al., 2012). However, the calculations of the RF are still subject to some specific assumptions, which we discuss in detail in the Supplement.

In general, we consider only the direct RF due to changes in the O_3 concentration. We calculate no RF due to changes in the methane concentration caused by anthropogenic emissions. These changes would lead to a negative RF due to decreased methane concentrations. Especially for shipping emissions, the negative RF due to methane can be larger compared to the positive ozone forcing (e.g. Myhre et al., 2011).

2.4 Simulation set-up

As an anthropogenic emissions inventory we chose the MACCity emission inventory (Granier et al., 2011), which follows the RCP8.5 scenario (Riahi et al., 2007, 2011) for the analysed period. The monthly varying anthropogenic emissions are represented on a grid with $0.5° \times 0.5°$ spatial resolution. The geographical distribution of the land transport (containing road traffic, inland navigation, and railways) and the shipping sector are shown in Fig. 1. Additionally, the total emissions of CO, NO_x, and NMHCs from the most important emission sectors are given in Table 2.

Three different simulations were conducted: one with all emissions (*BASE*), one with a 5 % decrease in the land transport emissions of NO_x, CO, and VOCs (*LTRA95*), and one with a 5 % decrease in the shipping emissions of NO_x, CO, and VOCs (*SHIP95*). The 5 % perturbation was chosen as previous studies showed that this small perturbation sufficiently minimizes the impact of the non-linearity of the chemistry on the results (e.g. Hoor et al., 2009; Grewe et al., 2010; Koffi et al., 2010).

All three simulations were equipped with the full tagging diagnostics. To quantify the contribution of the emission sources the tagging results of the *BASE* simulation are used. The simulations with a decrease in the land transport and shipping emissions were performed to allow for a direct comparison between the tagging and the perturbation method. The additional tagging diagnostics in the perturbed simulations allow for a more detailed investigation into the change in the ozone production (see Sect. 4).

In the present study we focus on the source regions of land transport and shipping emissions. Therefore we use the same geographical regions as defined by Righi et al. (2013) to investigate the contribution of these emissions. The regions are Europe (EU), North America (NA), and South-east Asia (SEA) for land transport and the North Atlantic Ocean (NAO), Indian Ocean (IO), and North Pacific Ocean (NPO) for the shipping emissions.

3 Contribution to ground-level ozone

First, we analyse the absolute amount of O_3 produced by land transport (tra) and ship (shp) exhaust as analysed with the tagging approach. Additionally, we indicate the relative contribution of O_3^{tra} and O_3^{shp} to near-ground-level O_3. For all quantities, multi-annual seasonal average values for December–February (DJF) and June–August (JJA) for the years 2006–2010 (for DJF starting with December 2005) were computed.

3.1 Land transport

Figure 2a and b show the seasonal average values of O_3^{tra} for DJF and JJA. The maximum absolute contribution for each hemisphere is simulated during local

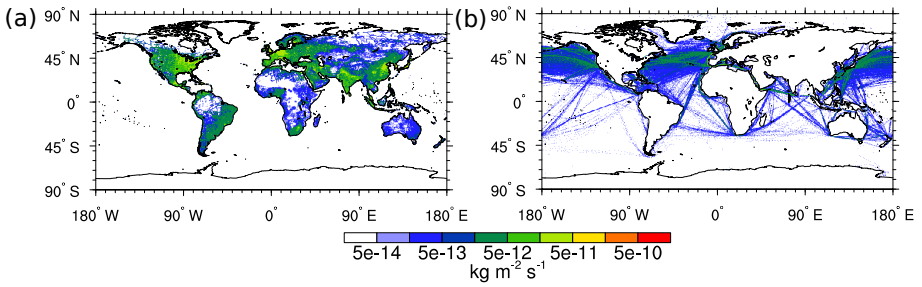

Figure 1. Average (2006–2010) flux of NO_x emissions (in kg (N) m^{-2} s^{-1}) from **(a)** land transport and **(b)** shipping.

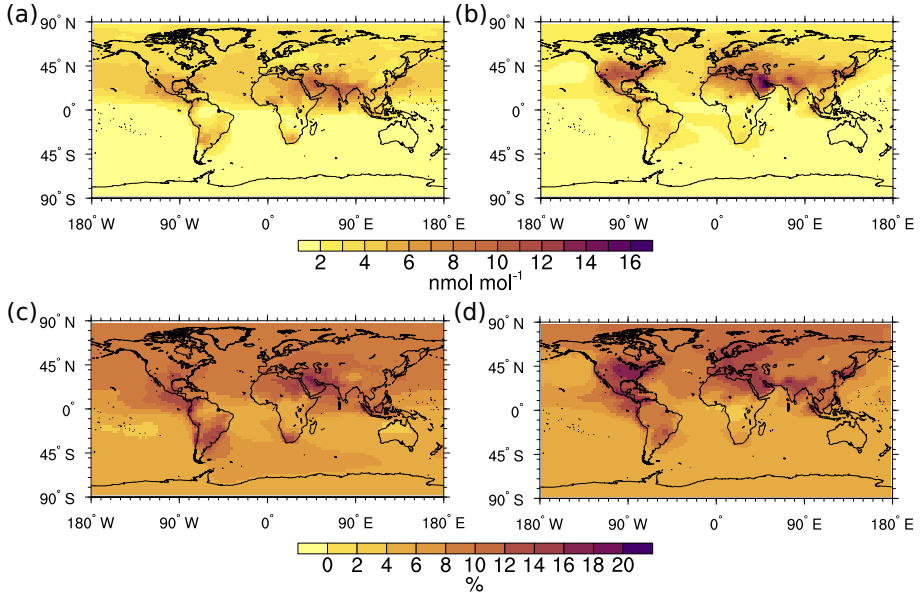

Figure 2. Seasonal average values of the absolute and relative contribution of O_3^{tra} to near-ground-level O_3. The upper row gives the absolute values (in nmol mol^{-1}) for winter (DJF, **a**) and summer (JJA, **b**). The lower row shows the DJF **(c)** and JJA **(d)** values of the contribution (in %).

summer conditions when the photochemistry is most effective. Most geographical locations of these maxima correspond to the regions with the largest land transport emissions. The largest absolute contributions of 8–14 nmol mol^{-1} are simulated during JJA in the Northern Hemisphere in North America (8–12 nmol mol^{-1}), Southern Europe (8–10 nmol mol^{-1}), the Arabian Peninsula (12–14 nmol mol^{-1}), India (8–10 nmol mol^{-1}), and South-east Asia (6–10 nmol mol^{-1}). In Asia the largest values are simulated around the Korean Peninsula rather than in China. This lower contribution of land transport emissions in China compared to Europe or North America is mainly caused by a much larger fraction of other anthropogenic emissions (e.g. industry and households) compared to land transport emissions (e.g. Righi et al., 2013). Accordingly, much more O_3 is produced in China by other anthropogenic emissions compared to land transport. The local maxima (4–6 nmol mol^{-1}) in the Southern Hemisphere are simulated during DJF when the photochemistry is most active. These maxima are located in South America and South Africa, corresponding to the regions with the largest land transport emissions in the Southern Hemisphere (see Fig. 1).

The relative contribution of O_3^{tra} to near-ground-level O_3 is depicted in Fig. 2c and d. Values of 14–16 % are simulated during DJF around the source regions in the Southern Hemisphere, but the absolute values in the Southern Hemisphere are lower compared to the Northern Hemisphere. The simulated relative contributions in the Northern Hemisphere during DJF are around 10 %. Only around the Arabian Peninsula are values of 14–16 % found. During JJA, these maxima increase to 14–18 % over North America and 12–16 % for the other hotspot regions in the Northern Hemisphere. One important reason for the change in the contribution from DJF to JJA (in the Northern Hemisphere) is the strong seasonal cycle of the anthropogenic non-traffic sector in our applied emission inventory, showing large emissions during winter and

Table 3. Summary of previous global model studies investigating the contribution and impact of land transport and road traffic emissions to ozone. Method denotes the percentage of the emissions reductions (perturbation). The other columns list the amount of land transport and road traffic emissions as well as the fraction (f) compared to the emissions used in the studies for NO_x (in Tg (N) a^{-1}), CO (in Tg (CO) a^{-1}), and NMHC (Tg (C) a^{-1}). The four rows on the right list the contribution of the land transport and road traffic categories as estimated by these studies in mixing ratios and/or percent. Where possible, we show the estimated contribution for the geographical regions defined in Sect. 2 and zonal average values (ZM). All contributions are given to near-ground-level ozone and for July conditions. The table is ordered by the year of publication. A "–" indicates missing information.

Study	Method	NO_x	fNO_x	CO	fCO	NMHC	fNMHC	NA	EU	SEA	ZM
								nmol mol^{-1}	nmol mol^{-1}	nmol mol^{-1}	nmol mol^{-1}
		Tg a^{-1}	%	Tg a^{-1}	%	Tg a^{-1}	%	%	%	%	%
GB03	100 %	10	24	207	14	–	–	–	–	–	–
								11–15	9–15	5–12	–
NM06	100 %	9	30[a]	196	36[a]	36	27[a]	5–20	5–15	5–10	–
								10–50	-5–25	5–50	–
NM06	100 %	9	30[a]	196	36[a]	36	27[a]		zonal mean		–
											up to 10
M07	100 %	9	24	237	–	27	5	–	–	–	–
								13–16	9–16	3–16	–
M07	100 %	9	24	237	–	27	5		zonal mean		up to 5
											up to 12
H09	5 %[b]	7	15	31	7	8	2	2–5[c]	2–6[c]	1–4[c]	–
								–	–	–	–
K10	5 %[b]	9	18	110	11	11	1	2–5	-1–5	1–3	–
								–	–	–	–
K10	100 %	9	18	110	11	11	1		zonal mean ground level		–
											up to 7
This study	tagging	10	20	152	16	17	3	3–14	3–13	2–11	
								6–19	8–18	5–16	
This study	tagging	10	20	152	16	17	3		zonal mean mid-latitudes NH		3–7
											9–11
This study	5 %[b]	10	20	152	16	17	3	1–9	−1 to 6	−1 to 5	–
								1–12	−3 to 9	−2 to 12	–
This study	5 %[b]	10	20	152	16	17	3		zonal mean mid-latitudes NH		2–4
											1–2

[a] Fraction only compared to all anthropogenic emissions. [b] Given values scaled to 100 %. [c] Given for average values from 800 hPa to the surface. Abbreviations: GB03 (Granier and Brasseur, 2003), N06 (Niemeier et al., 2006), M07 (Matthes et al., 2007), H09 (Hoor et al., 2009), K10 (Koffi et al., 2010).

lower emissions during summer. This leads to larger contributions of the anthropogenic non-traffic category during DJF compared to JJA.

To review estimates of the impact and contribution of previous studies and to compare the new results with previous values, Table 3 summarizes the amount of emissions as well as reported impacts and contributions of road traffic emissions from previous studies. So far, only the effects of road traffic emissions alone and not the total effect of land transport emissions have been investigated. With respect to the ozone precursors, road traffic emissions are the largest contributor to the land transport sector. The contributions of inland navigation and railways are smaller than the uncertainties of the road traffic emissions. Therefore we argue that our results of the land transport sector can be compared with previous studies considering only road traffic emissions (see also the amount of applied emissions in different studies in Table 3). In general, we are focusing on global studies only. The regional effects of road traffic emissions have also been investigated (e.g. Reis et al., 2000; Tagaris et al.,

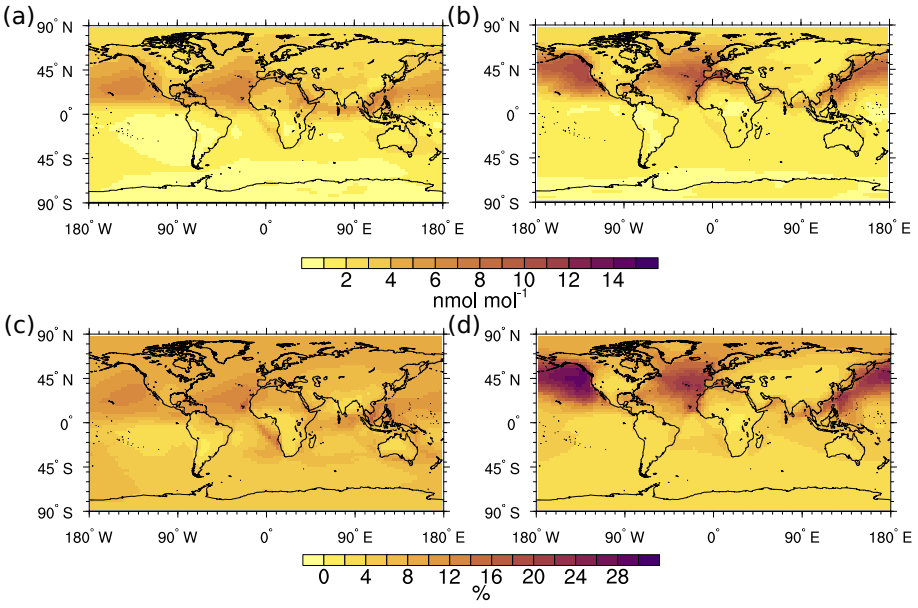

Figure 3. Seasonal average values of the absolute and relative contribution of O_3^{shp} to near-ground-level O_3. The upper row gives the absolute values (in nmol mol^{-1}) for DJF **(a)** and JJA **(b)**. The lower row shows the DJF **(c)** and JJA **(d)** values of the contribution (in %).

2015; Hendricks et al., 2017), but because of the coarse resolution of global models a quantitative comparison between the findings of regional studies with these global studies is not straightforward and probably not meaningful. Please note that we list our values in Table 3 for July conditions only to be comparable to other studies, since they also report values for July conditions. In addition, the impact of the land transport emissions was calculated with the results of the unperturbed and perturbed simulation (*BASE* minus *LTRA95*), which is scaled by 20 to estimate a 100 % perturbation. Figures showing the contribution and impact for the results of the present study are part of the Supplement.

Previously, the impact of road traffic emissions on ozone concentration has been investigated mainly using 100 and 5 % perturbation approaches. Most previous studies applied similar amounts of road traffic emissions as the present study used for land transport emissions (9–10 Tg a^{-1}). The fraction of NO_x emissions from road traffic compared to all emissions was largest in the studies of Granier and Brasseur (2003), Niemeier et al. (2006), and Matthes et al. (2007). These studies also applied the largest CO and VOC emissions, while the individual fractions vary across the studies.

In general, the results of all considered studies can be separated into three groups: (1) the largest values are reported by the present study (using the tagging approach) and by Niemeier et al. (2006). (2) Slightly lower values are given by Granier and Brasseur (2003) and Matthes et al. (2007), while (3) Hoor et al. (2009) and Koffi et al. (2010) report the lowest impact. These studies, however, differ not only in the emission inventories and models used, but also in the methods. The lowest values are in general reported by studies using the 5 % perturbation (scaled to 100 %), which is confirmed by our results using the same method. However, in general our simulation results show larger values compared to these previous findings. These differences are especially noticeable for the NA region. The differences might be caused by a different geographical distribution of the emissions or by larger CO and NMHC emissions in the emission inventory we applied. Further, differences in the atmospheric composition as simulated by the different models can influence the production rates of ozone, which might contribute to the differences in the simulated impacts.

The comparison of our results using the 5 % perturbation approach with the results using the tagging approach clearly confirms the known differences between estimates of the impact (perturbation) and contribution (tagging, e.g. Wang et al., 2009; Grewe et al., 2010, 2017; Emmons et al., 2012; Grewe et al., 2012; Clappier et al., 2017). Depending on the region, we find a difference of up to a factor of 4. The reason for this difference is investigated in more detail in Sect. 4.

Granier and Brasseur (2003), Niemeier et al. (2006), and Matthes et al. (2007), however, also used a perturbation approach, but report values which are more similar to our estimate using the tagging method. This is likely caused by the larger emissions applied in these studies compared to all other studies. Accordingly, the contribution of the road traffic emissions is underestimated by the perturbation method, but the larger emissions (and fraction) of the road traffic category lead to results which are similar to those estimated by the tagging method with smaller emissions. Of course other factors, like differences between the models, chemical mechanisms, geographical distribution, and different seasonal cy-

cles of the emissions, can also contribute to differences between the studies. The influence of these factors, however, is difficult to reveal.

3.2 Ship traffic

The absolute contributions of O_3^{shp} are shown in Fig. 3a and b. Similar to the shipping emissions (see Fig. 1), O_3^{shp} shows a strong north–south gradient. The maximum values in the Northern Hemisphere are located between 20 and 30° N during DJF ($\approx 6\,\mathrm{nmol\,mol^{-1}}$). These maxima move northwards during summer and increase in magnitude (10–12 $\mathrm{nmol\,mol^{-1}}$). This shift is caused by the increase in the photochemical activity in the Northern Hemisphere during summer. Most shipping emissions are located north of 30° N (see Fig. 1). With increasing ozone production during spring and summer, more O_3^{shp} near the regions with the largest emissions is formed compared to the regions of 20–30° N.

The largest values of the relative contribution of O_3^{shp} during DJF are around 14 % and are co-located with the regions of the largest values of O_3^{shp} (Fig. 3c). The maxima of the contribution increase during JJA to around 30 % in the north-western Pacific, while the values in the north-eastern Pacific are around 18–22 %. In the North Atlantic maximum contributions of 20 % are simulated (Fig. 3d).

Table 4 summarizes emissions and results of previous studies. In general most studies used similar global NO_x shipping emissions of around $4\,\mathrm{Tg\,(N)\,a^{-1}}$. The largest impact and contribution of shipping emissions is limited to distinct areas within the investigated geographical regions. Therefore the range of the given contributions and impacts within the geographical regions is large. The displacement between the regions of emissions and largest ozone production is well known (e.g. Endresen et al., 2003; Eyring et al., 2007) and mainly caused by complex interplay between NO_x emissions, transport of precursors, and ozone production.

As discussed for the impact and contribution of land transport emissions, there is a large discrepancy between the results using the 100 and the 5 % perturbation method. The studies using the 100 % method report impacts in the Atlantic and the Pacific in the range of 4–11 $\mathrm{nmol\,mol^{-1}}$ (corresponding to 12–40 %). In general previous studies report larger impacts in the Pacific compared to the Atlantic. Only Eyring et al. (2007) reported a larger perturbation in the North Atlantic compared to the Pacific, which can most likely be attributed to differences in the emission inventories, as Eyring et al. (2007) applied lower emissions in the North Pacific compared to the North Atlantic.

Hoor et al. (2009) and Koffi et al. (2010) report absolute impacts (5 % perturbation) in the range of 2–6 $\mathrm{nmol\,mol^{-1}}$. Our model results using a 5 % perturbation suggest somewhat larger impacts of around 2–8 $\mathrm{nmol\,mol^{-1}}$ (10–22 %) in the Atlantic and Pacific. Most likely this difference can be attributed to different shipping emissions applied.

The absolute contributions diagnosed using the tagging approach are larger and in the range of 3–11 $\mathrm{nmol\,mol^{-1}}$ (relative contribution: 10–33 %) in the Atlantic and Pacific. These contributions are at the lower end of the contributions reported by the studies using the 100 % approach. Compared to these studies, however, we applied the largest shipping emissions. Accordingly, a larger contribution compared to other studies can be expected. As the models and emission inventories used in all studies are very different we can only speculate about possible reasons.

One reason for this discrepancy might be the resolution of the model simulations. In previous studies a variety of resolutions were used (especially in the multi-model approaches by Eyring et al., 2007, and Hoor et al., 2009. Our horizontal resolution of $\approx 2.8°$ is at the finer end of most of these resolutions (only Dalsøren et al., 2009, used $\approx 1.875°$). A coarse resolution leads to a strong dilution of the shipping emissions. This effect can lead to an overestimation of the O_3 production (e.g. Wild and Prather, 2006). Our results are also influenced by this problem because a resolution of T42 dilutes the emissions over large areas. A model with finer resolution, effective emissions, or a plume model (e.g. Franke et al., 2008; Holmes et al., 2014) would likely diagnose smaller contributions. Another important contributor to the differences is the geographical distribution of ship emissions. If the ship tracks are too narrow, the ozone production might be suppressed (see discussion by Eyring et al., 2007). Further, differences in the seasonal cycles of emissions can contribute to the differences.

4 Comparing perturbation and tagging approach

As discussed in the previous section and by previous studies (e.g. Wang et al., 2009; Grewe et al., 2010), the perturbation approach, which is often used for source attribution, and the tagging approach lead to different results. To investigate this effect in more detail, ΔO_{3tra} (see Eq. 5) is analysed further. Here, we consider not only ground-level values, but also partial ozone columns integrated from the surface up to 850 hPa (called 850PC, in DU).

To quantify the difference between the perturbation and the tagging approach in more detail, Fig. 4a shows the 850PC of ΔO_{3tra}. Figure 4b shows the 850PC of (O_3^{tra}) for the *BASE* simulation. A qualitative comparison already indicates a relatively large difference between the impact (as estimated by the perturbation approach; Fig. 4a) and the contribution (by the tagging approach; Fig. 4b). Figure 4c shows the relative difference between the two quantities, indicating a difference between 40 and 80 %. The lowest differences are found in the Southern Hemisphere, while the difference is largest near the hotspot regions (North America, Europe, and South-east Asia). Here, the impact is up to a factor of 4 lower compared to the contribution (not shown). A large relative difference is also indicated in some regions near the Equator. In these

Table 4. Summary of previous global model studies investigating the contribution and impact of shipping emissions to ozone. Method denotes the percentage of the emissions reductions (perturbation). The other columns list the amount of shipping emissions and the fraction (f) compared to all emissions used in the studies for NO_x (in $Tg\,(N)\,a^{-1}$). The four rows on the right list the contribution of the shipping category as estimated by these studies in mixing ratios (upper row) and/or percent (lower row). Where possible, we show the estimated contribution for the geographical regions defined in Sect. 2 and zonal average values. For the geographical regions we give only the values larger than the background values. All contributions are given to near-ground-level ozone and for July conditions. The table is ordered by the year of publication. A "–" indicates missing information.

Study	Method	NO_x	$f\,NO_x$	Atlantic	Pacific	India	Zonal mean
				$nmol\,mol^{-1}$	$nmol\,mol^{-1}$	$nmol\,mol^{-1}$	$nmol\,mol^{-1}$
		$Tg\,a^{-1}$	%	%	%	%	%
ED03	100 %	4	8	4–12	4–11	3–4	–
				–	–	–	–
E07	100 %	3	11[a]	2–12	1–4	1–4	–
				12–36	12–24	12–18	–
E07	100 %	3	11[a]	zonal mean mid-latitudes NH			1–1.5
							–
H09	5 %[c]	4	10	2–4	2–3	1–2	–
				–	–	–	–
D09	100 %	5	–	–	–	–	–
				14–33	14–40	9–12	–
K10	5 %[c]	4	8	2–5	3–6	1–2	–
				–	–	–	–
K10	5 %[c]	4	8	zonal mean			up to 1.5
							–
K10	100 %	4	8	up to 8	up to 9	–	–
				–	–	–	–
K10	100 %	4	8	zonal mean			up to 3
							–
This study	tagging	6	12	3–9	4–11	2–5	–
				10–24	10–33	9–15	–
This study	tagging	6	12	zonal mean mid-latitudes NH			3–6
							10–15
This study	5 %[c]	6	12	2–8	2–7	1–4	–
				10–18	11–22	4–10	–
This study	5 %[c]	6	12	zonal mean mid-latitudes NH			2–4
							5–8

[a] No information available. [b] Fraction only compared to all anthropogenic emissions. [c] Given values scaled to 100 %. [d] Given for average values from 800 hPa to the surface. Abbreviations: ED03 (Endresen et al., 2003), E07 (Eyring et al., 2007), H09 (Hoor et al., 2009), D09 (Dalsøren et al., 2009), K10 (Koffi et al., 2010).

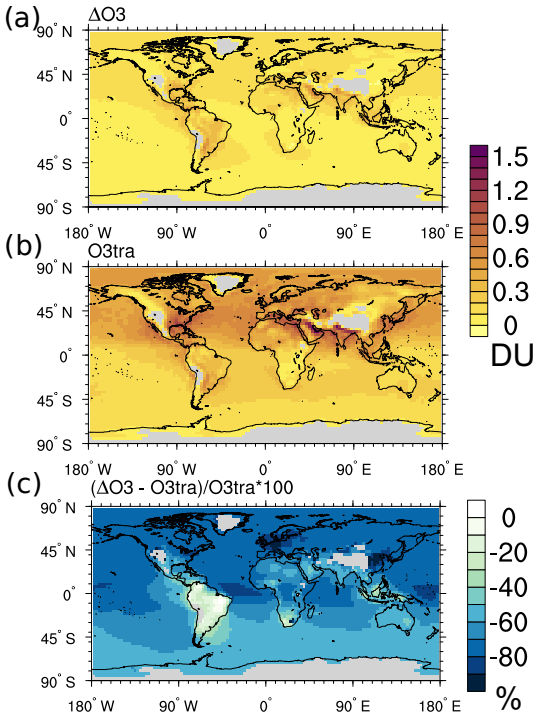

Figure 4. Multi-annual averages (2006–2010) of **(a)** ΔO_3 (impact) and **(b)** O_3^{tra} (contribution, both in DU) of the REF simulation and **(c)** the relative difference between the impact and the contribution of land transport emissions (in %). All values are calculated for the partial columns from the surface up to 850 hPa (850PC).

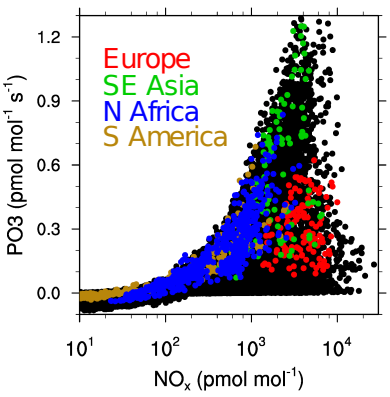

Figure 5. Dependency between NO_x mixing ratios and net O_3 production. The black dots represent monthly mean values at ground level for the year 2010 of every individual grid box. The individual colours indicate monthly average values during May–August (Northern Hemisphere) and November–February (Southern Hemisphere) for individual regions (defined as rectangular areas).

regions, however, the absolute difference is low. The only region where a difference below 20 % is simulated is in parts of South America. This difference between the impact and the contribution is not confined to the lower troposphere, but is present throughout the troposphere (additional figures showing zonal averaged impact and contributions are part of the Supplement).

To further investigate why the difference between impact and contribution largely change between the regions, the dependency between NO_x mixing ratios (caused by changes in the emissions) and the net O_3 production of the results for the year 2010 is analysed. Figure 5 shows this dependency for the whole globe (black) and some chosen areas (coloured dots). Generally the well-known dependency (e.g. Seinfeld and Pandis, 2006) between O_3 production and NO_x concentrations can be observed. In pristine regions a net loss of O_3 is present (first regime). With increasing NO_x mixing ratios the net O_3 production increases strongly (called a NO_x-limited regime). The production of O_3 decreases again with even larger NO_x values. In this third regime, however, the production of O_3 can be increased if the NMHC emissions are increased (called an NMHC-limited regime). Every dot represents a different grid box of the model with different meteorological conditions and background mixing ratios of CO, NMHC, etc. Therefore, the dependency between the NO_x mixing ratio and the net O_3 production differs for every grid box and is not given by one single function (which is the case for box model calculations with prescribed conditions).

In different regions of the world, O_3 production takes place in different chemical regimes depending on the amount of NO_x emissions. Therefore, the coloured dots highlight the individual relationship between the NO_x mixing ratio and the production of O_3 for four different regions. Depending on the chemical regime in the different regions, the ozone chemistry responds differently to the perturbation applied in the perturbation approach (e.g. Dahlmann et al., 2011).

Based on the results of the *REF* and *LTRA95* simulations, the ozone sensitivity is calculated with the tangent approach in accordance with Grewe et al. (2010) by solving a linear equation ($y = m \cdot (x - x_0) + b$; see the Supplement for additional figures). Here, x and y are the average NO_x mixing ratio and the net O_3 production (P_{O_3}), respectively, for a particular region. The m denotes the slope, which corresponds to an approximation of the derivative dP_{O_3} / dNO_x in the unperturbed simulation calculated by the difference in ozone production and NO_x mixing ratios in the unperturbed and perturbed simulation. The NO_x mean mixing ratio in the unperturbed simulation is $x_0 = NO_x^u$ and $b = P_{O_3}^u - dP_{O_3} / dNO_x \, NO_x^u$, where $P_{O_3}^u$ is the mean ozone production in the unperturbed simulation.

Based on the linearized ozone production ($P_{O_3}^{lin}$) calculated by the tangent approach, we define a saturation indicator Γ, which helps to analyse the ozone sensitivity further:

$$\Gamma = \frac{y \text{ axis intercept}}{y \text{ value of unperturbed simulation}} = \frac{P_{O_3}^{lin}(NO_x = 0)}{P_{O_3}^{lin}(NO_x = \text{ unperturbed})}. \quad (6)$$

Table 5. Comparison of Γ values (definition see text) between the four considered regions and an interpretation of these values.

	Γ	Interpretation
Europe	0.9	90 % of the O_3 reduction due to land transport emissions is compensated for by increased ozone production. Ozone contribution and impact differ largely.
South-east Asia	0.6	10 % reduction of land transport emissions will lead to a 4 % reduction in ozone due to increased ozone productivity. Ozone contribution and impact differ largely.
North Africa	0.4	Only small compensation effects; ozone contribution and impact differ only slightly.
South America	0.3	Land transport emission reduction almost scales with ozone reduction. Impact and contribution are almost equal.

Accordingly, Γ compares the production rate of ozone in the base case with unperturbed emissions (NO_x = unperturbed) to the approximated production rate of ozone if NO_x emissions are set to zero ($NO_x = 0$) and assuming a linear ozone chemistry. This value is a quantitative indicator of the chemical regime, showing how much an emission change in one specific sector is compensated for by increased ozone productivity in other sectors. $\Gamma = 1$ indicates a saturated behaviour of the ozone production; i.e. the ozone production does not change if emissions are changed ($P^{\mathrm{lin}}_{O_3}(NO_x = 0) = P^{\mathrm{lin}}_{O_3}(NO_x = \text{unperturbed})$). Accordingly, there is no ozone reduction because the change in the emissions is entirely compensated for by increasing ozone production efficiency of other emissions. $\Gamma > 1$ indicates an overcompensating effect; i.e. reduced NO_x emissions lead to an increase in the ozone production (corresponding to the VOC-limited regime). Finally, $\Gamma = 0$ indicates a linear response of the system (with a y intercept at zero). Accordingly, the ozone change introduced by an emission change is not compensated for by an increase in the ozone production efficiency. For $\Gamma = 0.5$ the ozone change is half compensated for by a change in the ozone production efficiency. In terms of the estimated derivative (dP_{O_3} / dNO_x), $\Gamma = 1$ corresponds to $dP_{O_3} / dNO_x = 0$, while $\Gamma > 1$ corresponds to $dP_{O_3} / dNO_x < 0$ and vice versa.

Table 5 lists the Γ values of the four different regions together with a brief interpretation of these values (additional information and figures concerning Γ are part of the Supplement). In general, only the regions North Africa and South America show a response of the O_3 chemistry which is close to linear ($\Gamma = 0.2$–0.3). As known (e.g. Wang et al., 2009; Grewe et al., 2010; Clappier et al., 2017) only for this linear case, the perturbation and the tagging approach lead to the same results (e.g. the contribution can be estimated using a perturbation approach). In all other regions the contribution is largely underestimated by the perturbation approach.

This underlines the importance of discriminating between tagging and perturbation. Clearly, both approaches answer different but equally important questions. The perturbation approach answers the question on the impact of an emission change. This approach is important to estimate effects due to mitigation measures (e.g. Williams et al., 2014). The tagging approach, in contrast, disentangles the ozone budget into the contributions of the individual emission sources and is important to investigate e.g. the contribution of the radiative forcing of individual emission sources (see Sect. 6) or to quantify the contribution of different emission sources to extreme ozone events. However, the tagging approach cannot be used to quantify the impact of an emission change, while the perturbation approach should not be used to quantify the contribution. As demonstrated, in regions where ozone responses more linearly to emission changes, both approaches differ slightly, but in regions where large emissions occur (e.g. Europe, South-east Asia) the perturbation approach largely underestimates the contributions and should not be used for source apportionment. However, if mitigation options are investigated the tagging approach should be combined with the perturbation approach (see next subsection).

4.1 Combining tagging and perturbation approach in mitigation studies

The tagging approach does not give any information about the sensitivity of the ozone chemistry with respect to a change in emissions. Accordingly, the success of an emission reduction, e.g. measured in terms of reduced ozone concentration, is evaluated using the perturbation approach. Wang et al. (2009) proposed first using a tagging simulation to estimate the sources which contribute most to ozone and therefore have the largest mitigation potential. However, we propose equipping all simulations (the unperturbed reference simulation and all simulations with changed emissions) with the tagging approach.

In this case the results of the perturbed simulations quantify the changes in ozone due to mitigation options. The tagging results provide additional information which is important to quantify the accountability of different emission sources to the ozone concentration or the associated radiative forcing. This additional information is important because the success of one specific mitigation option largely depends on the history of previous mitigations (Grewe et al., 2012).

To present the benefits of combining both methods in more detail, Fig. 6 sketches an idealized example of four different mitigation options. For each of the idealized mitigation options we assume a decrease in the emissions of one specific emission source by 10 arbitrary units. Mitigation option 1 reduces the land transport emissions, mitigation option 2 the

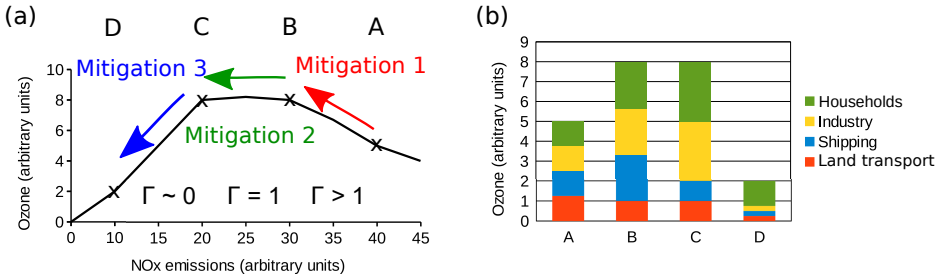

Figure 6. Idealized example explaining the difference in the perturbation and the tagging approach for the evaluation of mitigation increases. **(a)** The dependency between NO_x emissions and ozone (both in arbitrary units). Three different mitigation options are indicated by the coloured arrows. In addition, the approximate value of Γ (see text for definition) is given. **(b)** The contribution of the ozone concentration at the four marked points in **(a)**. In this example it is assumed that only four emission categories exist, emitting the same amount of emissions at point A.

shipping emissions, and mitigation option 3 the emissions from industry.

With respect to the ozone concentration (Fig. 6a) only mitigation option 3 is successful in largely reducing the ozone concentration. Having only the results with respect to the ozone concentration in mind, one could attribute the ozone change completely to the emissions change in the industry sector. From this point of view there would be no benefit to reducing land transport or shipping emissions.

However, if all simulations are additionally equipped with a tagging method, the contribution of the different emission sources to the ozone concentration is analysed (Fig. 6b). For each of the considered cases both the ozone concentration and the contribution of the different emission sources to this ozone concentration differ. This additional contribution analysis shows that even if due to mitigation option 1 the overall ozone concentration increases, the contribution of the road traffic emissions is lowered. At the same time, the contribution of all other emission sources, which are not changed, increase because the ozone production efficiency increases. However, if every emission source is made responsible for its individual contributions to ozone levels (for air quality mitigation purposes) or its individual contributions to ozone radiative forcing (for climate mitigation purposes), an obvious benefit exists for a specific emission source to reduce its emissions even if overall O_3 levels are only slightly reduced. This additional information is only available using the tagging approach.

This becomes even more clear if mitigation option 2 is considered in which the shipping emissions are reduced. The overall ozone concentration remains unchanged, as the ozone chemistry is in a saturated regime ($\Gamma = 1$). The contribution of the shipping emissions, however, decreases strongly, while the contribution of emissions from industry and household increases. Accordingly, the emission sources household and industry are more responsible for the ozone values and/or ozone radiative forcing, while the emission sources road traffic and shipping are less responsible. This puts pressure on these emission sources to reduce emissions of ozone precursors.

In mitigation option 3 the emissions of the industry sector are reduced. In this case, the response of the ozone concentration to emission changes is close to linear ($\Gamma \approx 0$) and the ozone concentration is reduced strongly. This emission reduction causes a reduction of the ozone production efficiency, leading not only to a reduction of the contribution of the industry emissions, but also to a further reduction of the contribution of all other sources.

The large effect of the ozone concentration for option 3 is only the effect of all previous mitigation options. In contrast, if the emissions from industry instead of the land transport emissions are reduced in mitigation option 1, this mitigation would have almost no effect on the ozone concentration. Clearly, the effect of one specific mitigation option strongly depends on the history of previous mitigation options. A combination of tagging and perturbation is a powerful tool for putting additional pressure on unmitigated emission sources because, even if the absolute ozone levels do not change, their shares in high ozone values (or radiative forcing) increase.

5 Analysis of the ozone budget

For more details about the influence of emissions from land transport and ship traffic on the ozone burden, we analysed the burden as well as the production and loss rates of O_3, O_3^{tra}, and O_3^{shp}. These analyses were performed globally and for the distinct geographical regions defined in Sect. 2. Please note that in our tagging method we distinguish only between different emission sources, but not between emission regions. Therefore, the budgets analysed for distinct geographical regions might not be solely influenced by regional emissions, but also by upwind sources.

The global total tropospheric burden of O_3 averaged for 2006–2010 is 318 Tg, which is in the range of 337 ± 23 Tg presented by Young et al. (2013) as a result of a multi-model

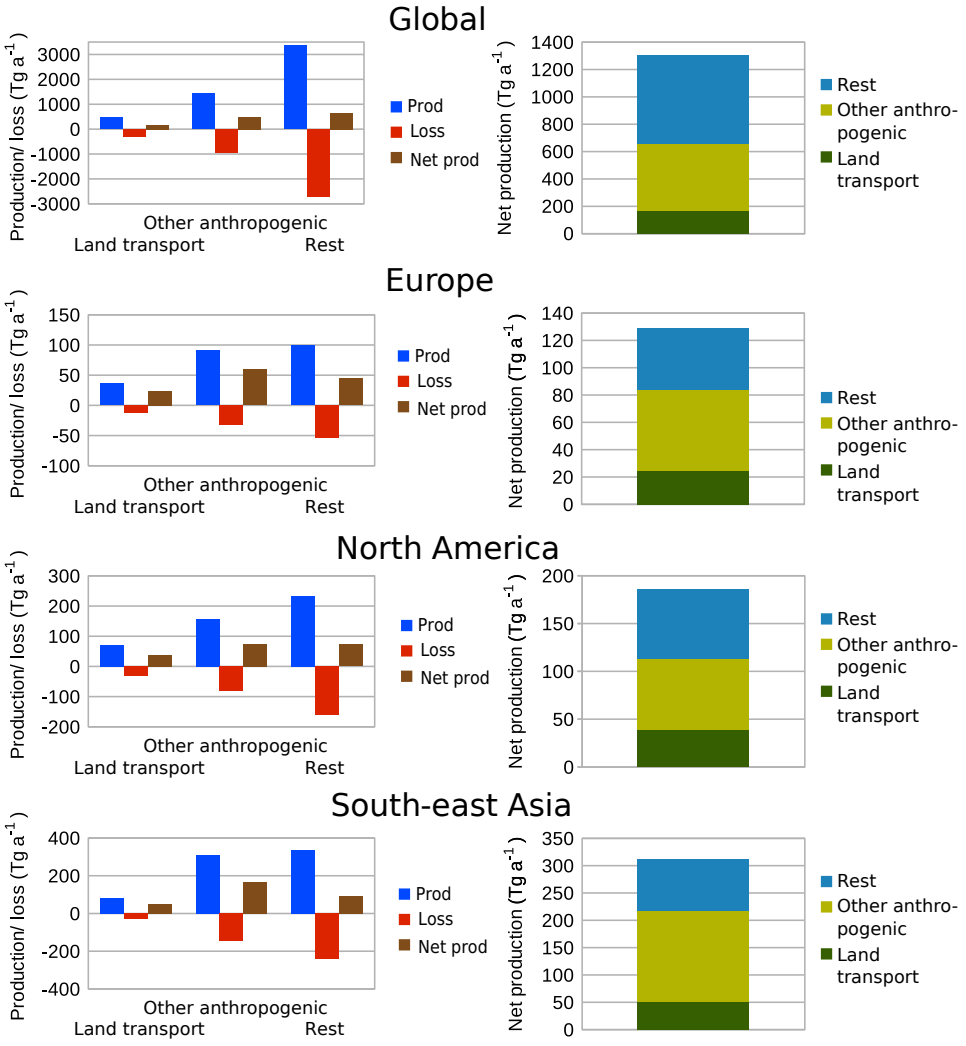

Figure 7. Production and loss rates of O_3 from different sectors (integrated up to 200 hPa and averaged for 2006–2010). The left side shows the individual production and loss rates as well as the net O_3 production, while the right side shows only the net production of the different sectors. For simplicity only land transport, other anthropogenic (shipping, anthropogenic non-traffic, and aviation), and the rest (all other tagging categories) are shown.

intercomparison, but please note that we used a fixed value of 200 hPa for the tropopause. Of this 318 Tg, globally 24 Tg is produced by land transport emissions, while 18 Tg is produced by emissions from shipping. The relative contribution of the burden of O_3^{tra} to the total ozone is thus around 8 % globally and 10 % in the regions Europe, North America, and South-east Asia. The relative contribution of the burden of O_3^{shp} is around 6 % globally and 8 % near the important source regions. The difference between the rather large contribution of the shipping emissions near ground level (see Sect. 3) and the much smaller contribution for the whole troposphere is mainly caused by the confinement of the contribution of shipping emissions to the lowermost troposphere (e.g. Eyring et al., 2007; Hoor et al., 2009).

To better understand the effect of land transport and shipping emissions on the atmospheric composition, we analysed the production and loss rates of O_3 from land transport and shipping emissions globally and for the individual regions. The corresponding numbers are shown in Figs. 7 and 8. Globally integrated production rates of 5274 Tg a^{-1} (averaged 2006–2010) are simulated, while the loss rate is 3972 Tg a^{-1}, leading to a net production of O_3 of 1301 Tg a^{-1}. Similar values of 5110 ± 606 Tg a^{-1} for production are reported by Young et al. (2013). The values of the loss are lower than reported by Young et al. (2013), but still within the spread of the different models (4668 ± 727 Tg a^{-1}; again note the different definition of the tropopause). Further, it is important to note that loss rates are not calculated consistently in all models presented by Young et al. (2013).

Globally a net production of 165 Tg a^{-1} from the land transport emissions is simulated, corresponding to a contribution of 13 % to the total net O_3 production. The contribu-

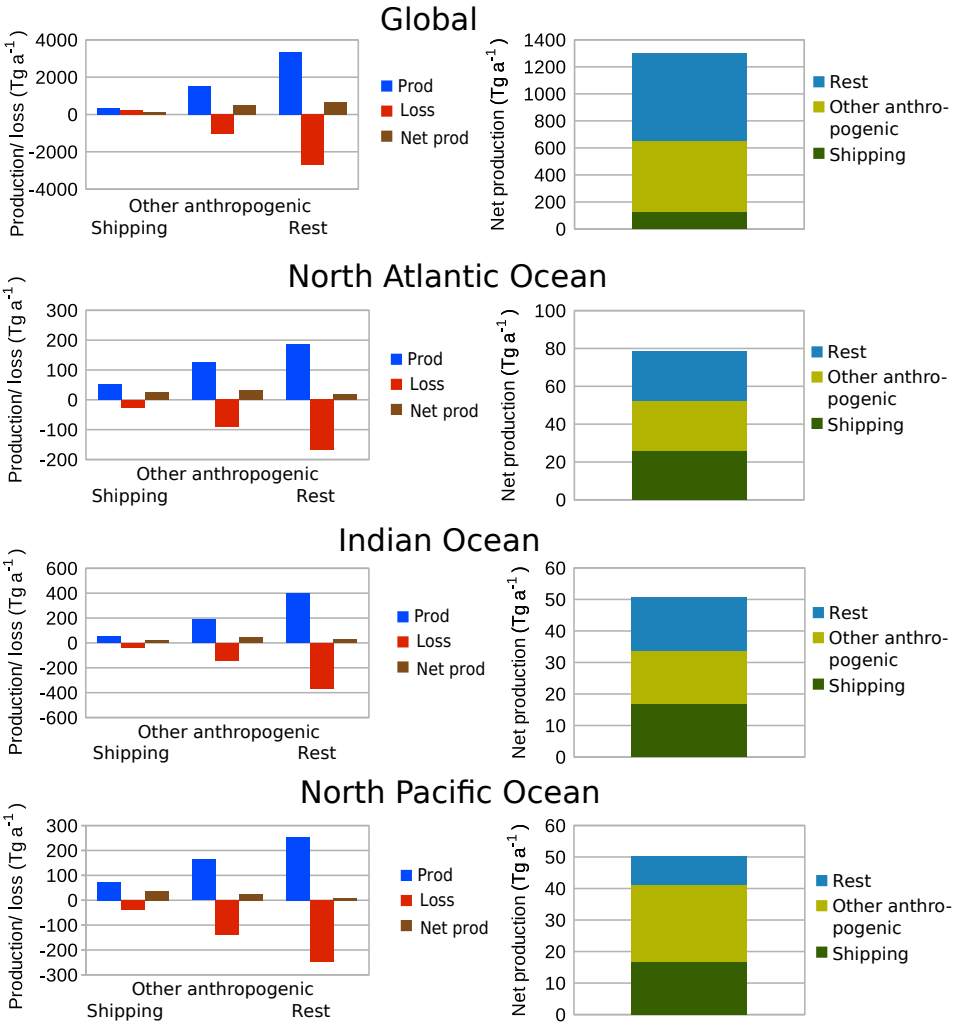

Figure 8. Production and loss rates of O_3 from different sectors (integrated up to 200 hPa and averaged for 2006–2010). The left side shows the individual production and loss rates as well as the net O_3 production, while the right side shows only the net production of the different sectors. For simplicity only shipping, other anthropogenic (land transport, anthropogenic non-traffic, and aviation), and the rest (all other tagging categories) are shown.

tion of the land transport category to the total net O_3 production near the source regions is 19 % over Europe (24 Tg a^{-1}), 21 % over North America (39 Tg a^{-1}), and 17 % over Southeast Asia (51 Tg a^{-1}).

A global net O_3 production of emissions from shipping of 129 Tg a^{-1} is simulated, corresponding to a contribution of 10 % to the total net O_3 production. Regionally, the importance of shipping emissions to the net O_3 production is much larger. Here contributions of 34 % over the North Atlantic (26 Tg a^{-1}), 19 % over the Indian Ocean (17 Tg a^{-1}), and 52 % over the North Pacific (36 Tg a^{-1}) are simulated. The larger relative contributions near the source regions compared to the land transport category are mainly caused by fewer or almost no emissions from other sources in the shipping region. Especially over land, other important sources, such as anthropogenic non-traffic and NO_x emissions from soil, decrease the relative importance of the land transport emissions. However, even near the source regions emissions from land transport contribute around 20 % to the net O_3 production in these regions.

6 Radiative forcing

We obtain a global net RF for land transport of $RF^{tagging}_{O3tra} = 92\,mW\,m^{-2}$. The shortwave RF is 32 mW m^{-2} and the longwave RF is 61 mW m^{-2}. The estimated RF of ship traffic is $RF^{tagging}_{O3shp} = 62\,mW\,m^{-2}$ and smaller than the land transport RF. The shortwave RF of ship emissions is 22 mW m^{-2} and the longwave is 40 mW m^{-2}. To review estimates of the RF of land transport and shipping emissions and to compare our results with previous estimates, Table 8 com-

Table 6. Burden of O_3 and O_3^{tra} integrated up to 200 hPa (in Tg). Average values for the period 2006–2010.

	O_3 (Tg)	O_3^{tra} (Tg)	Contribution O_3^{tra} (%)
Global	318	24	8
Europe	15	2	10
North America	21	2	10
South-east Asia	25	2	9

Table 7. Burden of O_3 (total) and O_3^{shp} (shipping) integrated up to 200 hPa (in Tg). Average values for the period 2006–2010.

	O_3 (Tg)	O_3^{shp} (Tg)	Contribution O_3^{shp} (%)
Global	318	18	6
North Atlantic Ocean	24	2	8
Indian Ocean	27	1	5
North Pacific Ocean	32	2	8

pares our results with previous studies. As noted in Sect. 2.3 only the RF of O_3 is shown, and the RF of changes due to CH_4 are not considered.

Most studies have estimated a lower RF of land transport and road traffic emissions of around $30\,mW\,m^{-2}$ using the perturbation approach. The review of Uherek et al. (2010) gives a range for the RF due to road traffic emissions of $50-(54\pm11)\,mW\,m^{-2}$. Compared to these values Dahlmann et al. (2011) give larger estimates of around $170\,mW\,m^{-2}$ using a NO_x-only tagging approach and larger global land transport NO_x emissions of roughly $13\,Tg\,(N)\,a^{-1}$. Comparing the RF per $Tg\,(N)\,a^{-1}$ Dahlmann et al. (2011) reported values of around $14\,mW\,m^{-2}\,Tg^{-1}\,(N)\,a$, while our estimates are around $10\,mW\,m^{-2}\,Tg^{-1}\,(N)\,a$.

Also for the RF due to shipping emissions previous estimates using the perturbation approach (around 20–$30\,mW\,m^{-2}$) are lower compared to our findings of around $60\,mW\,m^{-2}$. Only the tagging study by Dahlmann et al. (2011) report values which are more similar to our estimates ($49\,mW\,m^{-2}$), but this study used lower ship emissions of around $4\,Tg\,(N)\,a^{-1}$, while we applied roughly $6\,Tg\,(N)\,a^{-1}$. Accordingly, our results suggest an RF of $10\,mW\,m^{-2}\,Tg^{-1}\,(N)\,a$, while Dahlmann et al. (2011) reported values of around $12\,mW\,m^{-2}\,Tg^{-1}\,(N)\,a$. Clearly, the NO_x-only tagging used by Dahlmann et al. (2011) leads in general to a larger RF per Tg(N) compared to our NO_x and VOC tagging.

For a more detailed comparison we also calculated the RF due to land transport and shipping using the 5 % perturbation approach. By using this approach we estimate $RF_{\Delta O3tra}^{perturbation} = 24\,mW\,m^{-2}$ (scaled to 100 %) for land transport emissions and $RF_{\Delta O3shp}^{perturbation} = 22\,mW\,m^{-2}$ (scaled to 100 %) for shipping emissions. Both values are at the lower end of previous estimates of the RF using the perturbation approach. What is remarkable, however, is the difference of a factor of 3 to 4 between our results using the perturbation and the tagging approach despite using an identical model, identical emissions and a consistent calculation of the RF.

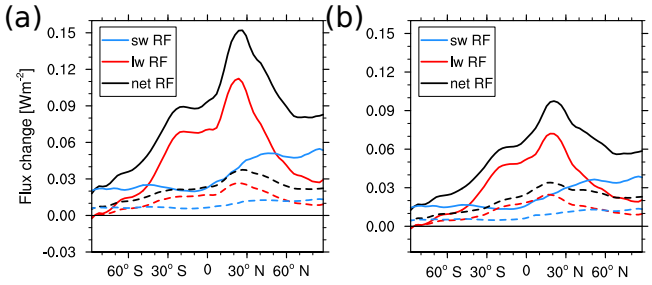

Figure 9. Zonal mean of shortwave, longwave, and net radiative O_3 forcing of **(a)** land transport and **(b)** ship traffic. The continuous lines give the results of the tagging method, and the dashed lines of the perturbation method.

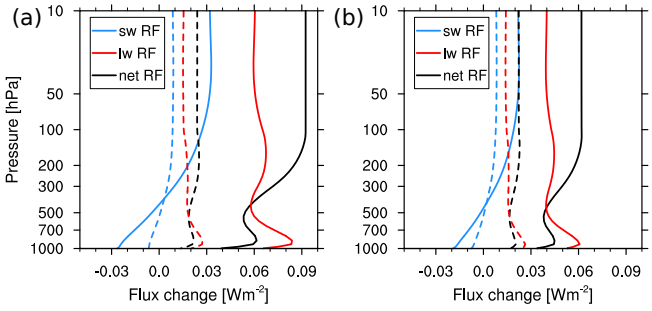

Figure 10. Vertical profile of globally averaged shortwave, longwave, and net radiative O_3 forcing of **(a)** land transport and **(b)** ship traffic. The continuous lines give the results of the tagging method, and the dashed lines of the perturbation method.

These results have important implications with respect to current estimates of the RF due to land transport (and shipping) emissions. The previous best estimates of an RF of $50-(54+11)\,mW\,m^{-2}$ by Uherek et al. (2010) are too low because these estimates are based on the perturbation approach. Previous studies using NO_x-only tagging (Dahlmann et al., 2011; Grewe et al., 2012) reported larger values of up to $170\,mW\,m^{-2}$, because the NO_x-only tagging does not consider the competing effects of NO_x and VOCs. Accordingly, our best estimate ($92\,mW\,m^{-2}$) of the RF due to land transport emissions lies between the two previous estimates. Compared to this Uherek et al. (2010) give an estimate of $171\,mW\,m^{-2}$ for the combined land transport CO_2 forcing, while Righi et al. (2015) report an RF of land transport aerosol on the order of -81 to $-12\,mW\,m^{-2}$.

The zonal averages of the shortwave, longwave, and net radiative forcing for land transport and ship traffic are shown

Table 8. Global estimates of the annually averaged radiative forcing due to O_3 caused by emissions of land transport and road traffic (global RF road) and ship emissions (global RF shp). Please note that individual studies use different methods for the calculation of the radiative forcing, e.g. some studies give instantaneous values, while other studies give stratospheric adjusted values (see last row).

Study	Method	Global RF road ($mW\,m^{-2}$)	Global RF shp ($mW\,m^{-2}$)	RF type
Endresen et al. (2003)	100 %	–	29	scaling of tropospheric ozone column change
Niemeier et al. (2006)	100 %	30 / 50 (Jan / Jul)	–	instantaneous at TP[e]
Eyring et al. (2007)	100 %	–	10 ± 2	instantaneous at TP[e] decreased by 22 %
Fuglestvedt et al. (2008)	100 %	54 ± 11	32 ± 9	stratospheric adjusted
Hoor et al. (2009)	5 %	28[a]	28[a]	–
Uherek et al. (2010)	review	$50 - (54 \pm 11)$	–	–
Dahlmann et al. (2011)	NO_x tagging	170[c]	49[c]	fixed dynamical heating
Dahlmann et al. (2011)	100 %	31[c]	–	fixed dynamical heating
Myhre et al. (2011)	5 %	31[a]	24[a]	
Grewe et al. (2012)	NO_x tagging	132[c]	–	fixed dynamical heating
Grewe et al. (2012)	100 %	24[c]	–	fixed dynamical heating
Holmes et al. (2014)	5 %	–	27[d]	–
This study	NO_x / VOC tagging	92	62	stratospheric adjusted
This study	5 %	24[a]	22[a]	stratospheric adjusted

[a] Scaled to 100 %. [b] For year 2000 conditions. [c] For year 1990 conditions. [d] Calculated by scaling the RF value of the "instant dilution" case for a change of $1\,Tg\,a^{-1}$ with the total amount of emissions used by Holmes et al. (2014). [e] Tropopause.

in Fig. 9. Solid (dashed) lines indicate the RF due to the tagging (perturbation) approach. The overall behaviour of RFs deduced by the tagging and perturbation approach compare very well. However, the RF obtained by the tagging approach is much larger than the RF obtained by the perturbation approach. In particular, the peak at around 20° N is more enhanced for the tagging approach. This is mainly caused by the larger O_3 shares in the upper troposphere where O_3 is most radiative active, as estimated by the tagging compared to the perturbation approach (see the Supplement for a figure showing the individual shares). In all cases, the longwave radiative forcing with ≈ 65 % dominates over the shortwave radiative forcing with ≈ 35 %. The overall shape of the net forcing corresponds to the tropospheric O_3^{tra} and O_3^{shp} column (not shown). In general, the RFs of land transport and ship traffic are largest in the Northern Hemisphere where most emissions occur. The overall behaviour of the RF zonal means compares quite well with that reported by Myhre et al. (2011); however, we simulate larger absolute values as discussed above.

Figure 10 shows the vertical profile of land transport and ship traffic radiative forcing for the tagging and perturbation approach. The tagging and perturbation approach show the same behaviour. However, the tagging approach has larger values. Most flux changes are simulated in the lower and middle troposphere (300–1000 hPa). Here, the shortwave RF is negative. In contrast, the longwave forcing is positive throughout the whole atmosphere. The vertical profiles correspond to the fraction of O_3^{tra} (and O_3^{shp}) to O_3: the fraction increases with height until it peaks at 850 hPa. In this regime, the largest flux changes occur as well. Above, it continuously decreases with height, and so do the flux changes.

7 Uncertainties

The general limitations of the tagging diagnostics applied in this study have been discussed by Grewe et al. (2017), and therefore we discuss here only the most important details. The mathematical method itself is accurate, but the implementation into the model requires some simplifications such as the introduction of chemical families. Grewe (2004) showed that the implementation of the NO_y family causes an error mainly after the first 12 h after major emissions and during this time may lead to an error caused by the family concept of up to 10 %. However, the analyses by Grewe (2004) have only been performed with a simple box model for the upper troposphere and considered only the NO_y family. Applied in an chemistry–climate model this error might be larger, especially with respect to the interplay of freshly emitted lightning NO_x emissions and oxidized anthropogenic emissions in the upper troposphere. A detailed quantification of this error is difficult. The implementation of the NMHC family causes an additional error, as the different reactivities are not explicitly taken into account. Currently this error cannot be quantified in detail. Other detailed VOC tagging approaches might help to quantify this error (e.g. Butler et al., 2018). Further, recent updates of the tagging scheme with respect to differences in the HO_x fam-

ily show an influence of 1–3 percentage points on the relative contribution of land transport and shipping emissions to ozone (Rieger et al., 2017). In general, we conclude that the error through the simplifications of the tagging method is estimated to be smaller than the errors arising from approximations applied in the global chemistry–climate models (physics and chemistry parameterizations, e.g. 20 % given by Eyring et al., 2007). For the future it would be very interesting to compare results from different tagging methods in more detail to have more quantitative information about the influence of the simplifications chosen by different methods. Other available tagging schemes, however, are based on kinetic approaches (Gromov et al., 2010), consider either only NO_x or VOC (e.g. Emmons et al., 2012; Butler et al., 2011), or are based on thresholds depending on whether the ozone chemistry is NO_x or VOC limited (e.g. Dunker et al., 2002; Kwok et al., 2015). The differences between the assumptions and the scales on which they are applied render a detailed comparison impossible.

However, the perturbation approach also faces an important limitation. The calculated impact largely depends on the magnitude of the chosen perturbation and the impacts are only valid for this specific perturbation (e.g. Hoor et al., 2009). In addition, the perturbation approach has a fundamental problem, namely a non-closed budget. This means that the sum of O_3 changes calculated for different perturbed emission sources (e.g. land transport and aviation) is not necessarily the total O_3 change if all emissions are reduced at the same time (e.g. Wang et al., 2009; Grewe et al., 2010).

Clearly, the largest sources of uncertainties are the emission inventories. Especially for source attribution, not only are the uncertainties of the emissions source of interest important, but also the uncertainties of all other emissions sources. As an example, the emissions of NO_x from soil are poorly constrained (e.g. Vinken et al., 2014). This is particularly problematic as part of the soil NO_x emissions take place in similar regions as the land transport emissions. Therefore NO_x from both emissions sources influences the ozone production concurrently.

With respect to the RF calculation our approach also uses some assumptions (for the tagging and the perturbation results) which we discuss in detail in Sect. 2.3 and the Supplement. Further, due to the large sensitivity of the RF to ozone in the upper troposphere, particularly lightning NO_x shows large radiative efficiency (Dahlmann et al., 2011) errors in the attribution due to the NO_y family approach (see above), which can lead here to an overestimated RF. This needs to be investigated in more detail in the future. We estimate a difference of 10–30 % between the RF calculations applied in this paper and the commonly used way of calculating RF by comparing the results of two simulations (for example, for pre-industrial times and the present day; for details see the Supplement). In general, these differences are smaller than the factor of 2–3 between the results of the tagging and the perturbation approach.

8 Summary and conclusion

We estimate the contribution of land transport and shipping emissions to tropospheric ozone for the first time with an advanced tagging method which considers not only NO_x, but also CO and VOC. Our results indicate a maximum contribution of land transport emissions during summer of up to 18 % to ground-level ozone in North America and 16 % in Southern Europe, which corresponds to up to 12 nmol mol^{-1} in North America and 10 nmol mol^{-1} in Europe.

The largest contribution of shipping emissions to ground-level ozone was simulated in the North Pacific Ocean and the North Atlantic Ocean. During summer, contributions of up to 30 % were simulated in the north-western Pacific Ocean, corresponding to up to 12 nmol mol^{-1}. In the North Atlantic Ocean contributions of up to 20 % during summer were calculated (up to 12 nmol mol^{-1}). The comparison with previous estimates clearly shows that the results strongly depend on the chosen method. Perturbation studies using a 5 % approach usually show the lowest contribution (scaled to 100 %) in the considered regions, while most 100 % perturbations and the tagging approach show the largest contributions.

Overall, emissions of land transport and ship traffic contribute 8 and 6 %, respectively, to the tropospheric ozone burden. Land transport emissions contribute around 20 % to the tropospheric ozone production near the source regions. The contribution of shipping emissions to the net ozone production near the source regions has values of up to 52 % in the North Pacific, which is even larger than the contribution of land transport emissions to the net production.

Using the tagging method we estimate a global average radiative forcing due to ozone caused by land transport emissions of 92 and 62 mW m^{-2} caused by shipping emissions. In general, radiative forcings are largest in the Northern Hemisphere and peak at around 30° N. While our estimates of the contribution of land transport and shipping emissions to tropospheric ozone are similar compared to previous studies using a 100 % perturbation, our estimates of the radiative forcing are larger by a factor of 2–3 compared to previous estimates using the perturbation method. As discussed in detail, this large difference compared to previous values is largely attributable to differences in the methodology leading to different estimates of the ozone shares attributable to land transport and shipping emissions. Previous estimates of the ozone RF due to land transport emissions using a NO_x-only tagging method, however, are too large as they do not consider the competing effects of NO_x and VOCs. Accordingly, 92 and 62 mW m^{-2} are the current best estimates of the ozone RF due to land transport and shipping emissions, as estimated using a source apportionment method.

Our results clearly indicate that it is important to differentiate between sensitivity methods (i.e. perturbation), which estimate the impact, and source apportionment methods (i.e. tagging), which estimate the contribution of emissions, be-

cause both approaches give answers to different questions. The perturbation approach measures the effect of an emission change, while only the tagging approach yields contributions of individual emission sources to ozone concentration. This difference is very important when interpreting the results, in particular when investigating the radiative forcing of individual emission categories. To investigate mitigation options, the tagging method cannot replace sensitivity (i.e. perturbation) studies and vice versa. However, we demonstrated that even if mitigation options are investigated, the sensitivity simulations should be equipped with a tagging method. The tagging approach provides very valuable additional information about the changes in the contributions to ozone due to the mitigation option, which puts additional pressure on unmitigated sources.

Data availability. Data are available in the Supplement.

The Supplement related to this article is available online at https://doi.org/10.5194/acp-18-5567-2018-supplement.

Competing interests. The authors declare that they have no conflict of interest.

Special issue statement. This article is part of the special issue "The Modular Earth Submodel System (MESSy) (ACP/GMD inter-journal SI)". It is not associated with a conference.

Acknowledgements. Mariano Mertens acknowledges funding from the DLR projects "Verkehr in Europa" and "Auswirkungen von NO_x". Furthermore, part of this work is funded by the DLR internal project "VEU2". We thank Robert Sausen, Mattia Righi (both DLR), and two anonymous reviewers for comments that improved this paper. Analysis and graphics for the data used were performed using the NCAR Command Language (version 6.4.0) software developed by UCAR/NCAR/CISL/TDD and available online: https://doi.org/10.5065/D6WD3XH5. Computational resources for the simulation were provided by the German Climate Computing Centre (DKRZ) in Hamburg (project 0617).

The article processing charges for this open-access publication were covered by a Research Centre of the Helmholtz Association.

Edited by: Tim Butler
Reviewed by: three anonymous referees

References

Butler, T., Lawrence, M., Taraborrelli, D., and Lelieveld, J.: Multi-day ozone production potential of volatile organic compounds calculated with a tagging approach, Atmos. Environ., 45, 4082–4090, https://doi.org/10.1016/j.atmosenv.2011.03.040, 2011.

Butler, T., Lupascu, A., Coates, J., and Zhu, S.: TOAST 1.0: Tropospheric Ozone Attribution of Sources with Tagging for CESM 1.2.2, Geosci. Model Dev. Discuss., https://doi.org/10.5194/gmd-2018-59, in review, 2018.

Clappier, A., Belis, C. A., Pernigotti, D., and Thunis, P.: Source apportionment and sensitivity analysis: two methodologies with two different purposes, Geosci. Model Dev., 10, 4245–4256, https://doi.org/10.5194/gmd-10-4245-2017, 2017.

Crutzen, P. J.: Photochemical reactions initiated by and influencing ozone in unpolluted tropospheric air, Tellus, 26, 47–57, https://doi.org/10.1111/j.2153-3490.1974.tb01951.x, 1974.

Dahlmann, K., Grewe, V., Ponater, M., and Matthes, S.: Quantifying the contributions of individual NO_x sources to the trend in ozone radiative forcing, Atmos. Environ., 45, 2860–2868, https://doi.org/10.1016/j.atmosenv.2011.02.071, 2011.

Dalsøren, S. B., Eide, M. S., Endresen, Ø., Mjelde, A., Gravir, G., and Isaksen, I. S. A.: Update on emissions and environmental impacts from the international fleet of ships: the contribution from major ship types and ports, Atmos. Chem. Phys., 9, 2171–2194, https://doi.org/10.5194/acp-9-2171-2009, 2009.

Deckert, R., Jöckel, P., Grewe, V., Gottschaldt, K.-D., and Hoor, P.: A quasi chemistry-transport model mode for EMAC, Geosci. Model Dev., 4, 195–206, https://doi.org/10.5194/gmd-4-195-2011, 2011.

Dee, D. P., Uppala, S. M., Simmons, A. J., Berrisford, P., Poli, P., Kobayashi, S., Andrae, U., Balmaseda, M. A., Balsamo, G., Bauer, P., Bechtold, P., Beljaars, A. C. M., van de Berg, L., Bidlot, J., Bormann, N., Delsol, C., Dragani, R., Fuentes, M., Geer, A. J., Haimberger, L., Healy, S. B., Hersbach, H., Hólm, E. V., Isaksen, L., Kållberg, P., Köhler, M., Matricardi, M., McNally, A. P., Monge-Sanz, B. M., Morcrette, J.-J., Park, B.-K., Peubey, C., de Rosnay, P., Tavolato, C., Thépaut, J.-N., and Vitart, F.: The ERA-Interim reanalysis: configuration and performance of the data assimilation system, Q. J. Roy. Meteor. Soc., 137, 553–597, https://doi.org/10.1002/qj.828, 2011.

Dietmüller, S., Jöckel, P., Tost, H., Kunze, M., Gellhorn, C., Brinkop, S., Frömming, C., Ponater, M., Steil, B., Lauer, A., and Hendricks, J.: A new radiation infrastructure for the Modular Earth Submodel System (MESSy, based on version 2.51), Geosci. Model Dev., 9, 2209–2222, https://doi.org/10.5194/gmd-9-2209-2016, 2016.

Dunker, A. M., Yarwood, G., Ortmann, J. P., and Wilson, G. M.: Comparison of source apportionment and source sensitivity of ozone in a three-dimensional air quality model, Environ. Sci. Technol., 36, 2953–2964, https://doi.org/10.1021/es011418f, 2002.

Emmons, L. K., Hess, P. G., Lamarque, J.-F., and Pfister, G. G.: Tagged ozone mechanism for MOZART-4, CAM-chem and other chemical transport models, Geosci. Model Dev., 5, 1531–1542, https://doi.org/10.5194/gmd-5-1531-2012, 2012.

Endresen, Ø., Sørgård, E., Sundet, J. K., Dalsøren, S. B., Isaksen, I. S. A., Berglen, T. F., and Gravir, G.: Emission from international sea transportation and environ-

mental impact, J. Geophys. Res.-Atmos., 108, 4560, https://doi.org/10.1029/2002JD002898, 2003.

Eyring, V., Stevenson, D. S., Lauer, A., Dentener, F. J., Butler, T., Collins, W. J., Ellingsen, K., Gauss, M., Hauglustaine, D. A., Isaksen, I. S. A., Lawrence, M. G., Richter, A., Rodriguez, J. M., Sanderson, M., Strahan, S. E., Sudo, K., Szopa, S., van Noije, T. P. C., and Wild, O.: Multi-model simulations of the impact of international shipping on Atmospheric Chemistry and Climate in 2000 and 2030, Atmos. Chem. Phys., 7, 757–780, https://doi.org/10.5194/acp-7-757-2007, 2007.

Eyring, V., Isaksen, I. S., Berntsen, T., Collins, W. J., Corbett, J. J., Endresen, O., Grainger, R. G., Moldanova, J., Schlager, H., and Stevenson, D. S.: Transport impacts on atmosphere and climate: shipping, Atmos. Environ., 44, 4735–4771, https://doi.org/10.1016/j.atmosenv.2009.04.059, 2010.

Fowler, D., Pilegaard, K., Sutton, M., Ambus, P., Raivonen, M., Duyzer, J., Simpson, D., Fagerli, H., Fuzzi, S., Schjoerring, J., Granier, C., Neftel, A., Isaksen, I., Laj, P., Maione, M., Monks, P., Burkhardt, J., Daemmgen, U., Neirynck, J., Personne, E., Wichink-Kruit, R., Butterbach-Bahl, K., Flechard, C., Tuovinen, J., Coyle, M., Gerosa, G., Loubet, B., Altimir, N., Gruenhage, L., Ammann, C., Cieslik, S., Paoletti, E., Mikkelsen, T., Ro-Poulsen, H., Cellier, P., Cape, J., Horvàth, L., Loreto, F., Niinemets, U., Palmer, P., Rinne, J., Misztal, P., Nemitz, E., Nilsson, D., Pryor, S., Gallagher, M., Vesala, T., Skiba, U., Brüggemann, N., Zechmeister-Boltenstern, S., Williams, J., O'Dowd, C., Facchini, M., de Leeuw, G., Flossman, A., Chaumerliac, N., and Erisman, J.: Atmospheric composition change: ecosystems–atmosphere interactions, Atmos. Environ., 43, 5193–5267, https://doi.org/10.1016/j.atmosenv.2009.07.068, 2009.

Franke, K., Eyring, V., Sander, R., Hendricks, J., Lauer, A., and Sausen, R.: Toward effective emissions of ships in global models, Meteorol. Z., 17, 117–129, https://doi.org/10.1127/0941-2948/2008/0277, 2008.

Fuglestvedt, J., Berntsen, T., Myhre, G., Rypdal, K., and Skeie, R. B.: Climate forcing from the transport sectors, P. Natl. Acad. Sci. USA, 105, 454–458, https://doi.org/10.1073/pnas.0702958104, 2008.

Granier, C. and Brasseur, G. P.: The impact of road traffic on global tropospheric ozone, Geophys. Res. Lett., 30, 1086, https://doi.org/10.1029/2002GL015972, 2003.

Granier, C., Bessagnet, B., Bond, T., D'Angiola, A., van der Gon, H. D., Frost, G., Heil, A., Kaiser, J., Kinne, S., Klimont, Z., Kloster, S., Lamarque, J.-F., Liousse, C., Masui, T., Meleux, F., Mieville, A., Ohara, T., Raut, J.-C., Riahi, K., Schultz, M., Smith, S., Thompson, A., Aardenne, J., Werf, G., and Vuuren, D.: Evolution of anthropogenic and biomass burning emissions of air pollutants at global and regional scales during the 1980–2010 period, Climatic Change, 109, 163–190, 2011.

Grewe, V.: Technical Note: A diagnostic for ozone contributions of various NO_x emissions in multi-decadal chemistry-climate model simulations, Atmos. Chem. Phys., 4, 729–736, https://doi.org/10.5194/acp-4-729-2004, 2004.

Grewe, V.: A generalized tagging method, Geosci. Model Dev., 6, 247–253, https://doi.org/10.5194/gmd-6-247-2013, 2013.

Grewe, V., Dameris, M., Fichter, C., and Sausen, R.: Impact of aircraft NO_x emissions. Part 1: Interactively coupled climate-chemistry simulations and sensitivities to climate-chemistry feedback, lightning and model resolution, Meteorol. Z., 11, 177–186, https://doi.org/10.1127/0941-2948/2002/0011-0177, 2002.

Grewe, V., Tsati, E., and Hoor, P.: On the attribution of contributions of atmospheric trace gases to emissions in atmospheric model applications, Geosci. Model Dev., 3, 487–499, https://doi.org/10.5194/gmd-3-487-2010, 2010.

Grewe, V., Dahlmann, K., Matthes, S., and Steinbrecht, W.: Attributing ozone to NO_x emissions: implications for climate mitigation measures, Atmos. Environ., 59, 102–107, https://doi.org/10.1016/j.atmosenv.2012.05.002, 2012.

Grewe, V., Tsati, E., Mertens, M., Frömming, C., and Jöckel, P.: Contribution of emissions to concentrations: the TAGGING 1.0 submodel based on the Modular Earth Submodel System (MESSy 2.52), Geosci. Model Dev., 10, 2615–2633, https://doi.org/10.5194/gmd-10-2615-2017, 2017.

Gromov, S., Jöckel, P., Sander, R., and Brenninkmeijer, C. A. M.: A kinetic chemistry tagging technique and its application to modelling the stable isotopic composition of atmospheric trace gases, Geosci. Model Dev., 3, 337–364, https://doi.org/10.5194/gmd-3-337-2010, 2010.

Guenther, A., Hewitt, C., E., D., Fall, R. G., C., Graedel, T., Harley, P., Klinger, L., Lerdau, M., McKay, W., Pierce, T., S., B., Steinbrecher, R., Tallamraju, R., Taylor, J., and Zimmermann, P.: A global model of natural volatile organic compound emissions, J. Geophys. Res., 100, 8873–8892, 1995.

Haagen-Smit, A. J.: Chemistry and physiology of Los Angeles smog, Ind. Eng. Chem., 44, 1342–1346, https://doi.org/10.1021/ie50510a045, 1952.

Hansen, J., Sato, M., and Ruedy, R.: Radiative forcing and climate response, J. Geophys. Res.-Atmos., 102, 6831–6864, https://doi.org/10.1029/96JD03436, 1997.

Hendricks, J., Righi, M., Dahlmann, K., Gottschaldt, K.-D., Grewe, V., Ponater, M., Sausen, R., Heinrichs, D., Winkler, C., Wolfermann, A., Kampffmeyer, T., Friedrich, R., Klötzke, M., and Kugler, U.: Quantifying the climate impact of emissions from land-based transport in Germany, Transport. Res. D-Tr. E., https://doi.org/10.1016/j.trd.2017.06.003, online first, 2017.

Holmes, C. D., Prather, M. J., and Vinken, G. C. M.: The climate impact of ship NO_x emissions: an improved estimate accounting for plume chemistry, Atmos. Chem. Phys., 14, 6801–6812, https://doi.org/10.5194/acp-14-6801-2014, 2014.

Hoor, P., Borken-Kleefeld, J., Caro, D., Dessens, O., Endresen, O., Gauss, M., Grewe, V., Hauglustaine, D., Isaksen, I. S. A., Jöckel, P., Lelieveld, J., Myhre, G., Meijer, E., Olivie, D., Prather, M., Schnadt Poberaj, C., Shine, K. P., Staehelin, J., Tang, Q., van Aardenne, J., van Velthoven, P., and Sausen, R.: The impact of traffic emissions on atmospheric ozone and OH: results from QUANTIFY, Atmos. Chem. Phys., 9, 3113–3136, https://doi.org/10.5194/acp-9-3113-2009, 2009.

Jöckel, P., Tost, H., Pozzer, A., Brühl, C., Buchholz, J., Ganzeveld, L., Hoor, P., Kerkweg, A., Lawrence, M. G., Sander, R., Steil, B., Stiller, G., Tanarhte, M., Taraborrelli, D., van Aardenne, J., and Lelieveld, J.: The atmospheric chemistry general circulation model ECHAM5/MESSy1: consistent simulation of ozone from the surface to the mesosphere, Atmos. Chem. Phys., 6, 5067–5104, https://doi.org/10.5194/acp-6-5067-2006, 2006.

Jöckel, P., Kerkweg, A., Pozzer, A., Sander, R., Tost, H., Riede, H., Baumgaertner, A., Gromov, S., and Kern, B.: Development

cycle 2 of the Modular Earth Submodel System (MESSy2), Geosci. Model Dev., 3, 717–752, https://doi.org/10.5194/gmd-3-717-2010, 2010.

Jöckel, P., Tost, H., Pozzer, A., Kunze, M., Kirner, O., Brenninkmeijer, C. A. M., Brinkop, S., Cai, D. S., Dyroff, C., Eckstein, J., Frank, F., Garny, H., Gottschaldt, K.-D., Graf, P., Grewe, V., Kerkweg, A., Kern, B., Matthes, S., Mertens, M., Meul, S., Neumaier, M., Nützel, M., Oberländer-Hayn, S., Ruhnke, R., Runde, T., Sander, R., Scharffe, D., and Zahn, A.: Earth System Chemistry integrated Modelling (ESCiMo) with the Modular Earth Submodel System (MESSy) version 2.51, Geosci. Model Dev., 9, 1153–1200, https://doi.org/10.5194/gmd-9-1153-2016, 2016.

Kerkweg, A., Sander, R., Tost, H., and Jöckel, P.: Technical note: Implementation of prescribed (OFFLEM), calculated (ONLEM), and pseudo-emissions (TNUDGE) of chemical species in the Modular Earth Submodel System (MESSy), Atmos. Chem. Phys., 6, 3603–3609, https://doi.org/10.5194/acp-6-3603-2006, 2006.

Koffi, B., Szopa, S., Cozic, A., Hauglustaine, D., and van Velthoven, P.: Present and future impact of aircraft, road traffic and shipping emissions on global tropospheric ozone, Atmos. Chem. Phys., 10, 11681–11705, https://doi.org/10.5194/acp-10-11681-2010, 2010.

Kwok, R. H. F., Baker, K. R., Napelenok, S. L., and Tonnesen, G. S.: Photochemical grid model implementation and application of VOC, NO_x, and O_3 source apportionment, Geosci. Model Dev., 8, 99–114, https://doi.org/10.5194/gmd-8-99-2015, 2015.

Lawrence, M. G. and Crutzen, P. J.: Influence of NO_x emissions from ships on tropospheric photochemistry and climate, Nature, 402, 167–170, 1999.

Lelieveld, J. and Dentener, F. J.: What controls tropospheric ozone?, J. Geophys. Res.-Atmos., 105, 3531–3551, https://doi.org/10.1029/1999JD901011, 2000.

Matthes, S., Grewe, V., Sausen, R., and Roelofs, G.-J.: Global impact of road traffic emissions on tropospheric ozone, Atmos. Chem. Phys., 7, 1707–1718, https://doi.org/10.5194/acp-7-1707-2007, 2007.

Monks, P. S.: Gas-phase radical chemistry in the troposphere, Chem. Soc. Rev., 34, 376–395, https://doi.org/10.1039/B307982C, 2005.

Monks, P. S., Archibald, A. T., Colette, A., Cooper, O., Coyle, M., Derwent, R., Fowler, D., Granier, C., Law, K. S., Mills, G. E., Stevenson, D. S., Tarasova, O., Thouret, V., von Schneidemesser, E., Sommariva, R., Wild, O., and Williams, M. L.: Tropospheric ozone and its precursors from the urban to the global scale from air quality to short-lived climate forcer, Atmos. Chem. Phys., 15, 8889–8973, https://doi.org/10.5194/acp-15-8889-2015, 2015.

Myhre, G., Shine, K., Rädel, G., Gauss, M., Isaksen, I., Tang, Q., Prather, M., Williams, J., van Velthoven, P., Dessens, O., Koffi, B., Szopa, S., Hoor, P., Grewe, V., Borken-Kleefeld, J., Berntsen, T., and Fuglestvedt, J.: Radiative forcing due to changes in ozone and methane caused by the transport sector, Atmos. Environ., 45, 387–394, https://doi.org/10.1016/j.atmosenv.2010.10.001, 2011.

Myhre, G., Shindell, D., Bréon, F.-M., Collins, W., Fuglestvedt, J., Huang, J., Koch, D., Lamarque, J.-F., Lee, D., Mendoza, B., Nakajima, T., Robock, A., Stephens, G., Takemura, T., and Zhang, H.: Anthropogenic and natural radiative forcing, 659–740, https://doi.org/10.1017/CBO9781107415324.018, available at: www.climatechange2013.org (last access: 18 April 2018), Cambridge University Press, 2013.

Naik, V., Voulgarakis, A., Fiore, A. M., Horowitz, L. W., Lamarque, J.-F., Lin, M., Prather, M. J., Young, P. J., Bergmann, D., Cameron-Smith, P. J., Cionni, I., Collins, W. J., Dalsøren, S. B., Doherty, R., Eyring, V., Faluvegi, G., Folberth, G. A., Josse, B., Lee, Y. H., MacKenzie, I. A., Nagashima, T., van Noije, T. P. C., Plummer, D. A., Righi, M., Rumbold, S. T., Skeie, R., Shindell, D. T., Stevenson, D. S., Strode, S., Sudo, K., Szopa, S., and Zeng, G.: Preindustrial to present-day changes in tropospheric hydroxyl radical and methane lifetime from the Atmospheric Chemistry and Climate Model Intercomparison Project (ACCMIP), Atmos. Chem. Phys., 13, 5277–5298, https://doi.org/10.5194/acp-13-5277-2013, 2013.

Niemeier, U., Granier, C., Kornblueh, L., Walters, S., and Brasseur, G. P.: Global impact of road traffic on atmospheric chemical composition and on ozone climate forcing, J. Geophys. Res., 111, D09301, https://doi.org/10.1029/2005JD006407, 2006.

Reis, S., Simpson, D., Friedrich, R., Jonson, J., Unger, S., and Obermeier, A.: Road traffic emissions – predictions of future contributions to regional ozone levels in Europe, Atmos. Environ., 34, 4701–4710, https://doi.org/10.1016/S1352-2310(00)00202-8, 2000.

Riahi, K., Grübler, A., and Nakicenovic, N.: Scenarios of long-term socio-economic and environmental development under climate stabilization, Technol. Forecast. Soc., 74, 887–935, https://doi.org/10.1016/j.techfore.2006.05.026, 2007.

Riahi, K., Rao, S., Krey, V., Cho, C., Chirkov, V., Fischer, G., Kindermann, G., Nakicenovic, N., and Rafaj, P.: RCP 8.5 – a scenario of comparatively high greenhouse gas emissions, Climatic Change, 109, 33, https://doi.org/10.1007/s10584-011-0149-y, 2011.

Rieger, V. S., Mertens, M., and Grewe, V.: An advanced method of contributing emissions to short-lived chemical species (OH and HO_2): The TAGGING 1.1 submodel based on the Modular Earth Submodel System (MESSy 2.53), Geosci. Model Dev. Discuss., https://doi.org/10.5194/gmd-2017-227, in review, 2017.

Righi, M., Hendricks, J., and Sausen, R.: The global impact of the transport sectors on atmospheric aerosol: simulations for year 2000 emissions, Atmos. Chem. Phys., 13, 9939–9970, https://doi.org/10.5194/acp-13-9939-2013, 2013.

Righi, M., Eyring, V., Gottschaldt, K.-D., Klinger, C., Frank, F., Jöckel, P., and Cionni, I.: Quantitative evaluation of ozone and selected climate parameters in a set of EMAC simulations, Geosci. Model Dev., 8, 733–768, https://doi.org/10.5194/gmd-8-733-2015, 2015.

Roeckner, E., Brokopf, R., Esch, M., Giorgetta, M., Hagemann, S., Kornblueh, L., Manzini, E., Schlese, U., and Schulzweida, U.: Sensitivity of simulated climate to horizontal and vertical resolution in the ECHAM5 Atmosphere Model, J. Climate, 19, 3771–3791, https://doi.org/10.1175/jcli3824.1, 2006.

Sander, R., Baumgaertner, A., Gromov, S., Harder, H., Jöckel, P., Kerkweg, A., Kubistin, D., Regelin, E., Riede, H., Sandu, A., Taraborrelli, D., Tost, H., and Xie, Z.-Q.: The atmospheric chemistry box model CAABA/MECCA-3.0, Geosci. Model Dev., 4, 373–380, https://doi.org/10.5194/gmd-4-373-2011, 2011.

Schumann, U. and Huntrieser, H.: The global lightning-induced nitrogen oxides source, Atmos. Chem. Phys., 7, 3823–3907, https://doi.org/10.5194/acp-7-3823-2007, 2007.

Seinfeld, J. H. and Pandis, S. N.: Atmospheric Chemistry and Physics: From Air Pollution to Climate Change, Wiley, 2006.

Stevenson, D. S., Dentener, F. J., Schultz, M. G., Ellingsen, K., van Noije, T. P. C., Wild, O., Zeng, G., Amann, M., Atherton, C. S., Bell, N., Bergmann, D. J., Bey, I., Butler, T., Cofala, J., Collins, W. J., Derwent, R. G., Doherty, R. M., Drevet, J., Eskes, H. J., Fiore, A. M., Gauss, M., Hauglustaine, D. A., Horowitz, L. W., Isaksen, I. S. A., Krol, M. C., Lamarque, J.-F., Lawrence, M. G., Montanaro, V., Müller, J.-F., Pitari, G., Prather, M. J., Pyle, J. A., Rast, S., Rodriguez, J. M., Sanderson, M. G., Savage, N. H., Shindell, D. T., Strahan, S. E., Sudo, K., and Szopa, S.: Multimodel ensemble simulations of present-day and near-future tropospheric ozone, J. Geophys. Res., 111, D08301, https://doi.org/10.1029/2005JD006338, 2006.

Stuber, N., Sausen, R., and Ponater, M.: Stratosphere adjusted radiative forcing calculations in a comprehensive climate model, Theor. Appl. Climatol., 68, 125–135, 2001.

Tagaris, E., Sotiropoulou, R. E. P., Gounaris, N., Andronopoulos, S., and Vlachogiannis, D.: Effect of the Standard Nomenclature for Air Pollution (SNAP) categories on air quality over Europe, Atmosphere, 6, 1119, https://doi.org/10.3390/atmos6081119, 2015.

Tost, H., Jöckel, P., Kerkweg, A., Sander, R., and Lelieveld, J.: Technical note: A new comprehensive SCAVenging submodel for global atmospheric chemistry modelling, Atmos. Chem. Phys., 6, 565–574, https://doi.org/10.5194/acp-6-565-2006, 2006.

Uherek, E., Halenka, T., Borken-Kleefeld, J., Balkanski, Y., Berntsen, T., Borrego, C., Gauss, M., Hoor, P., Juda-Rezler, K., Lelieveld, J., Melas, D., Rypdal, K., and Schmid, S.: Transport impacts on atmosphere and climate: land transport, Atmos. Environ., 44, 4772–4816, https://doi.org/10.1016/j.atmosenv.2010.01.002, 2010.

Vinken, G. C. M., Boersma, K. F., Maasakkers, J. D., Adon, M., and Martin, R. V.: Worldwide biogenic soil NO_x emissions inferred from OMI NO_2 observations, Atmos. Chem. Phys., 14, 10363–10381, https://doi.org/10.5194/acp-14-10363-2014, 2014.

von Kuhlmann, R., Lawrence, M. G., Pöschl, U., and Crutzen, P. J.: Sensitivities in global scale modeling of isoprene, Atmos. Chem. Phys., 4, 1–17, https://doi.org/10.5194/acp-4-1-2004, 2004.

Wang, Z. S., Chien, C.-J., and Tonnesen, G. S.: Development of a tagged species source apportionment algorithm to characterize three-dimensional transport and transformation of precursors and secondary pollutants, J. Geophys. Res.-Atmos., 114, d21206, https://doi.org/10.1029/2008JD010846, 2009.

Wild, O. and Prather, M. J.: Global tropospheric ozone modeling: Quantifying errors due to grid resolution, J. Geophys. Res.-Atmos., 111, d11305, https://doi.org/10.1029/2005JD006605, 2006.

Williams, J., Hodnebrog, Ø., van Velthoven, P., Berntsen, T., Dessens, O., Gauss, M., Grewe, V., Isaksen, I., Olivié, D., Prather, M., and Tang, Q.: The influence of future non-mitigated road transport emissions on regional ozone exceedences at global scale, Atmos. Environ., 89, 633–641, https://doi.org/10.1016/j.atmosenv.2014.02.041, 2014.

World Health Organization: Health Aspect of Air Pollution with Particulate Matter, Ozone and Nitrogen Dioxide, World Health Organization, Bonn, 2003.

Yienger, J. J. and Levy, H.: Empirical model of global soil-biogenic NO_x emissions, J. Geophys. Res.-Atmos., 100, 11447–11464, https://doi.org/10.1029/95JD00370, 1995.

Young, P. J., Archibald, A. T., Bowman, K. W., Lamarque, J.-F., Naik, V., Stevenson, D. S., Tilmes, S., Voulgarakis, A., Wild, O., Bergmann, D., Cameron-Smith, P., Cionni, I., Collins, W. J., Dalsøren, S. B., Doherty, R. M., Eyring, V., Faluvegi, G., Horowitz, L. W., Josse, B., Lee, Y. H., MacKenzie, I. A., Nagashima, T., Plummer, D. A., Righi, M., Rumbold, S. T., Skeie, R. B., Shindell, D. T., Strode, S. A., Sudo, K., Szopa, S., and Zeng, G.: Pre-industrial to end 21st century projections of tropospheric ozone from the Atmospheric Chemistry and Climate Model Intercomparison Project (ACCMIP), Atmos. Chem. Phys., 13, 2063–2090, https://doi.org/10.5194/acp-13-2063-2013, 2013.